

# Thermal and Kinematic Sunyaev-Z'eldovich Effects: Five Decades of Uncovering Relics

*Louis Penafiel  
Cornell University*

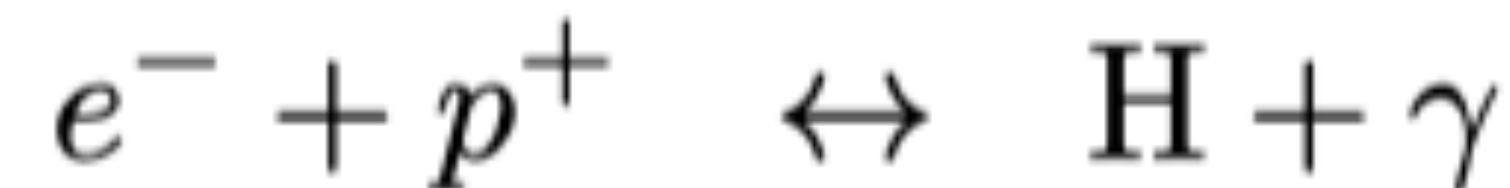
*A Exam Presentation  
10 May 2020*

# Outline

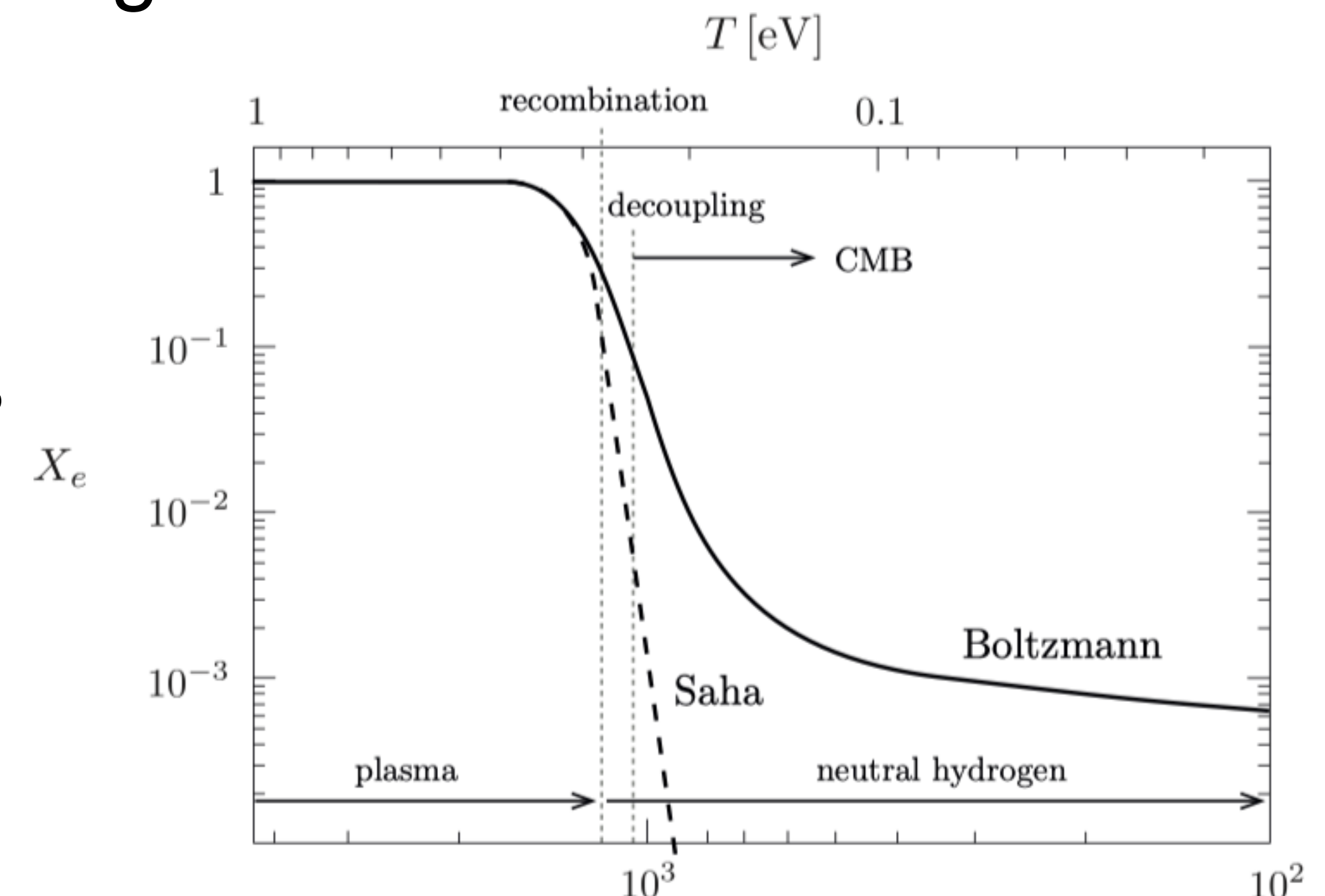
- **Background**
- **Thermal Sunyaev-Z'eldovich (tSZ) Effect**
- **Kinematic Sunyaev-Z'eldovich (kSZ) Effect**
- **Previous measurements**
- **Current experiments and future forecasts**

# Recombination — Electrons

- As the early universe was cooling down,  $T > 1 \text{ eV}$ , it was still composed of plasma of free electrons and nuclei
- Baryons and photons were in equilibrium through reactions such as



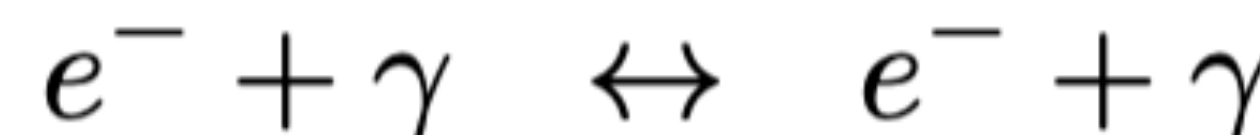
- As temperatures decrease,  $T < 1 \text{ eV}$ , there's not enough energy to keep this equilibrium, and more and more electrons are combined with protons to form hydrogen



Source: Baumann's Cosmology Notes

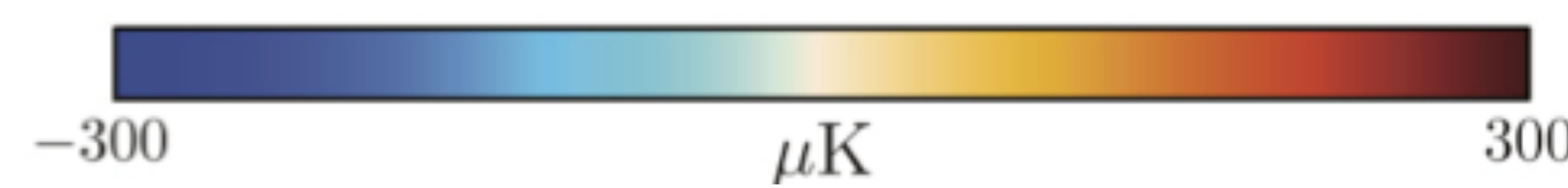
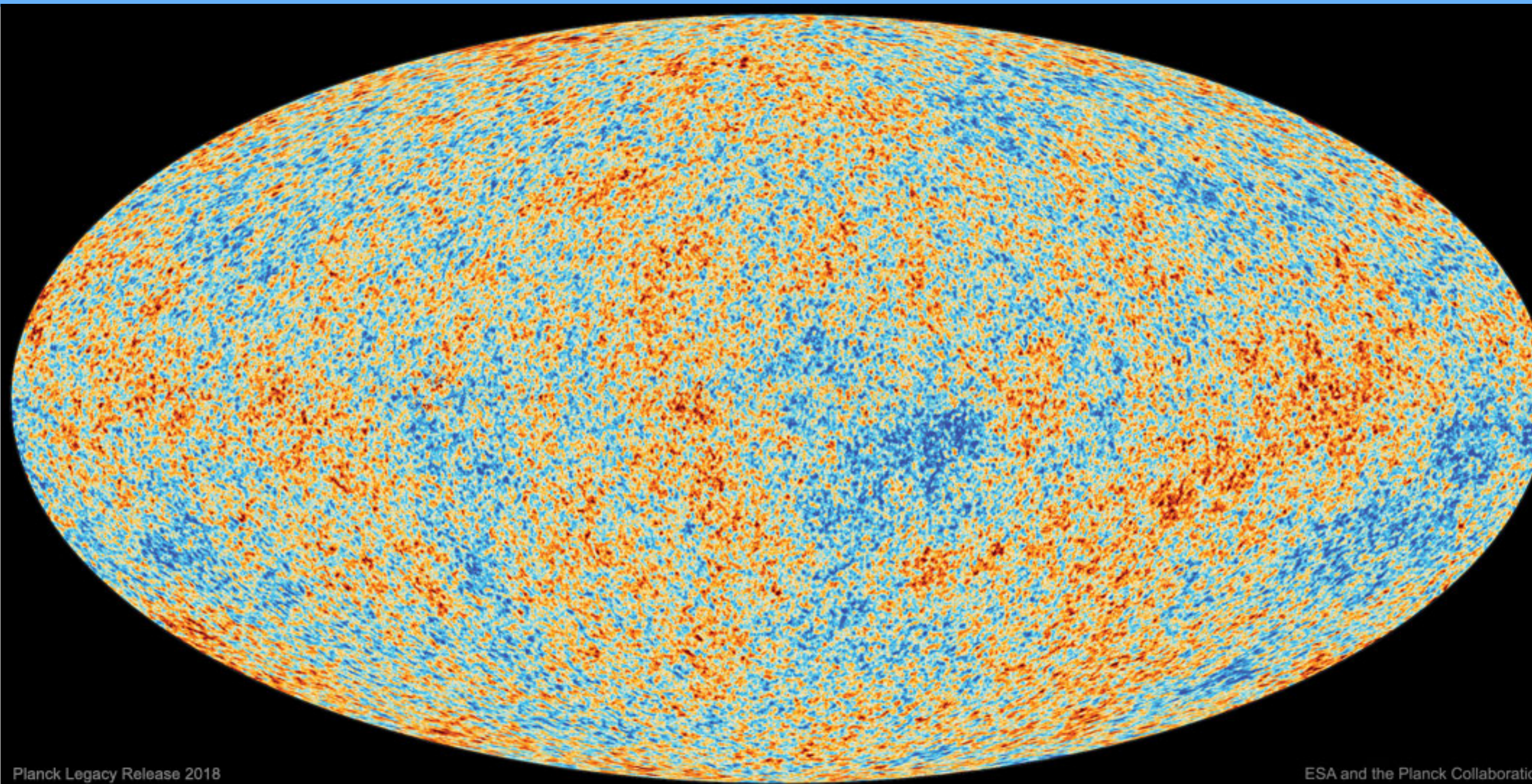
# Recombination — Photons

- In turn, the photons are most strongly couple to the plasma with electrons through Compton scattering



- As the density of free electrons decrease, this interaction rate also decreases
- In this way, the photons decouple from electrons, around 380,000 years after the Big Bang, and stream freely, which we detect today as the Cosmic Microwave Background (CMB)

# Cosmic Microwave Background



The CMB was first discovered in 1965 by Penzias and Wilson.

With multiple decades of advancements, the temperature of the CMB was found to be  $2.7260 \pm 0.0013$  K.

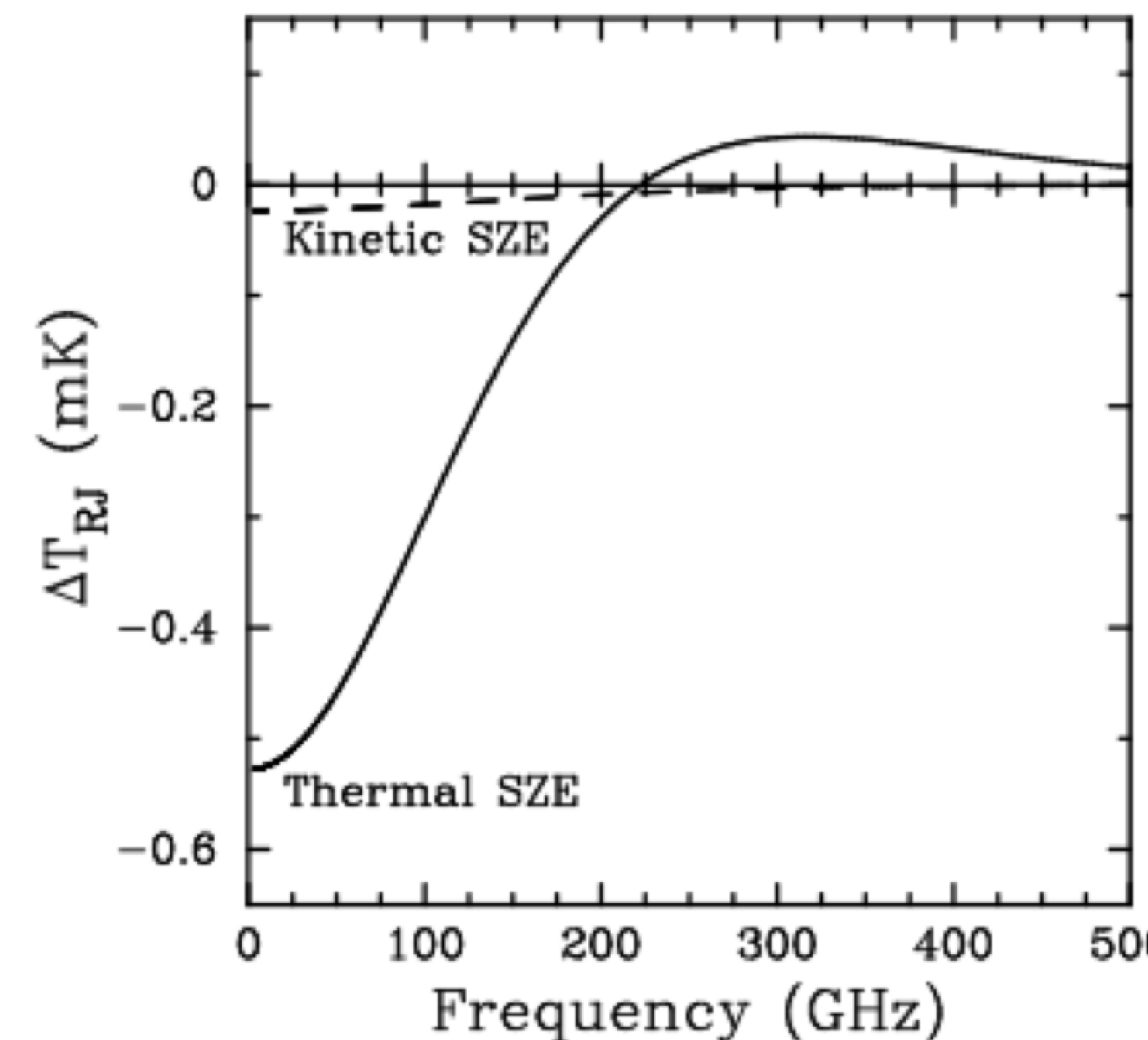
The observations are also more fine-grained to detect anisotropies: primary and **secondary**

# Sunyaev Z'eldovich Effect

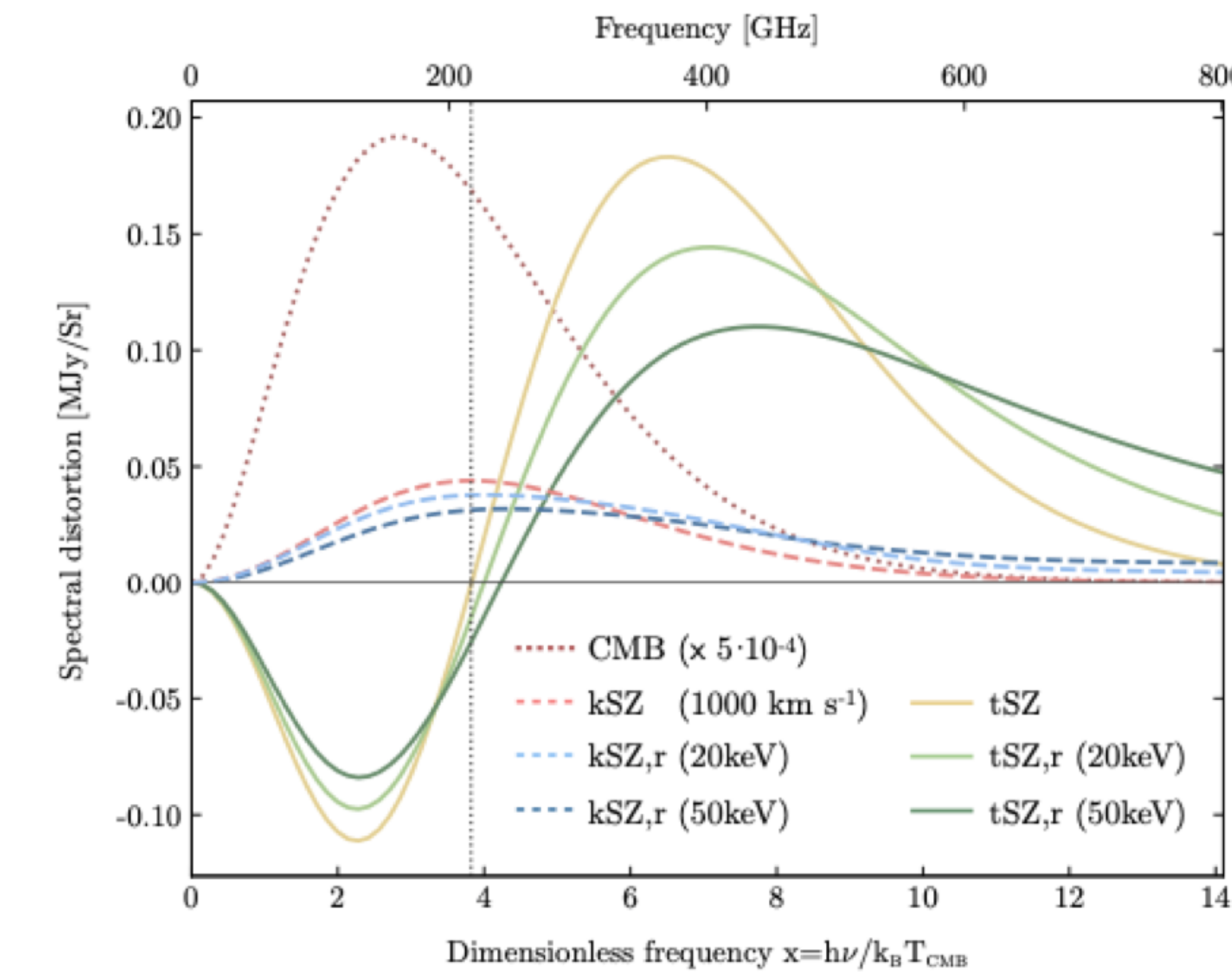
- These free streaming CMB photons can interact with free, high energy electrons, via Compton scattering, that can lead to small spectral distortions in the CMB (SZ 1970, 1972)
- These are called the Sunyaev-Z'eldovich (SZ) effects, and there are 5 types
  1. **Thermal SZ (tSZ)**: scattering with electrons in the intracluster medium (ICM)
  2. **Kinematic SZ (kSZ)**: scattering with electrons that move with large bulk velocities
  3. Relativistic SZ (rSZ): relativistic corrections may need to be taken into account
  4. Non-thermal SZ (ntSZ): contributions from thermal and magnetic fields
  5. Polarized SZ (pSZ): small polarization effect from scattering

# Spectral Distortions in the CMB

1. **Thermal SZ (tSZ)**: scattering with electrons in the intracluster medium (ICM)
2. **Kinematic SZ (kSZ)**: scattering with electrons that move with large bulk velocities



Source: Carlstrom et al. (2002)



Source: Mroczkowski et al. (2019)

# tSZ Effect — Theory

- Interaction boosts the CMB photon energy ( $\sim 1$  mK).
- Derivation based on original papers and previous reviews  
Define a dimensionless frequency  $x \equiv h\nu/k_B T_{CMB}$   
The tSZ effect expressed as a temperature change is given by

$$\frac{\Delta T_{tSZ}}{T_{CMB}} = f(x)y = f(x) \int n_e \frac{k_B T_e}{m_e c^2} \sigma_T d\ell = f(x) \frac{P_e}{m_e c^2} \int \sigma_T d\ell$$

- We used the equation for pressure due to electrons in the last relation,  $P_e = n_e k_B T_e$
- $y$  is the Compton-y parameter, which is equal to the optical depth times the fractional energy per scattering
  - $\sigma_T$  is the Thompson cross-section
  - $n_e$ ,  $T_e$ ,  $m_e c^2$  are the number density, temperature, and rest energy of electrons

# tSZ Effect — Theory

$$\frac{\Delta T_{tSZ}}{T_{CMB}} = f(x)y = f(x) \int n_e \frac{k_B T_e}{m_e c^2} \sigma_T d\ell = f(x) \frac{P_e}{m_e c^2} \int \sigma_T d\ell$$

As seen above, the frequency dependence for the tSZ comes in the function

$$f(x) = \left( x \frac{e^x + 1}{e^x - 1} - 4 \right) (1 + \delta_{tSZ}(x, T_e))$$

where  $\delta_{tSZ}$  is the relativistic correction to the frequency dependence. We can take the derivative with respect to the temperature, to get the distortion into units of specific density, yielding

$$\Delta I_{tSZ} = g(x) I_0 y$$

$$g(x) = \frac{x^4 e^x}{(e^x - 1)^2} \left( x \frac{e^x + 1}{e^x - 1} - 4 \right) (1 + \delta_{tSZ}(x, T_e))$$

# tSZ Effect — Applications

- There are several features of the tSZ that make it relevant for finding clusters and understanding the evolution of the universe, including
  1. Independence in redshift
  2. Unique and small ( $\sim 1$  mK) spectral signature compared to CMB
  3. **Integrated tSZ flux is proportional to total thermal energy of the cluster**
- The last feature is evident when we integrate the tSZ signal over the solid angle of the cluster,  $d\Omega = dA/D_A^2$ , yielding

$$Y_{SZ} = \int \Delta T_{tSZ} d\Omega \propto \frac{N_e \langle T_e \rangle}{D_A^2} \propto \frac{M \langle T_e \rangle}{D_A^2}$$

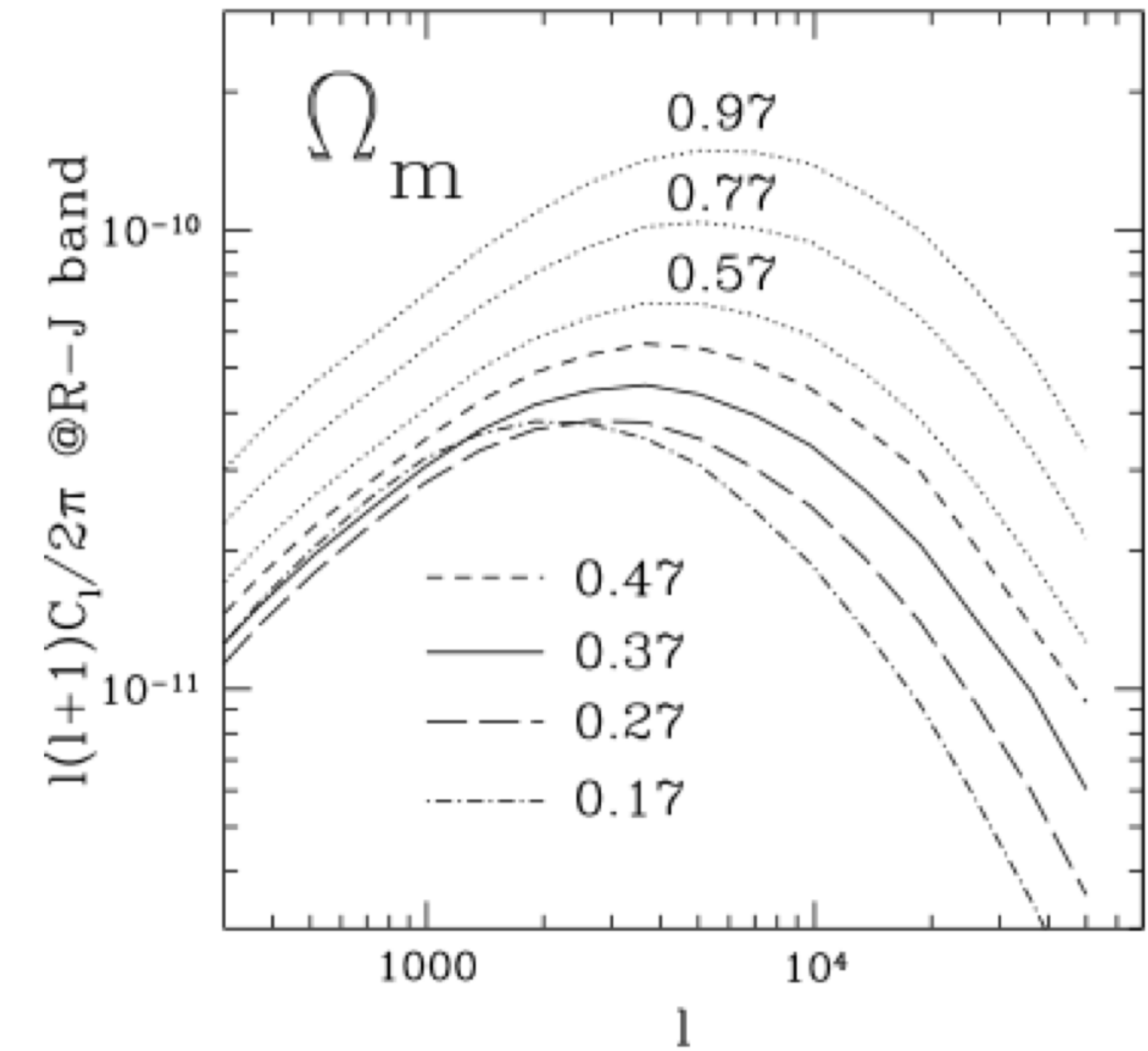
where  $\langle T_e \rangle$  is the mean electron temperature,  $M$  is the mass of the cluster,  $D_A$  is the angular diameter distance, and  $N_e$  is the total number of electrons

# tSZ Effect — Matter abundance

Most of the baryons contained in the ICM are confined to the cluster potential

Can approximate the universal baryon density ratio to the cluster baryon density ratio. With a determination of  $\Omega_B$ , we can find the matter abundance,  $\Omega_M$ , from the ratio

Alternatively, there's a strong dependence between the angular power spectra of the tSZ and  $\Omega_M$

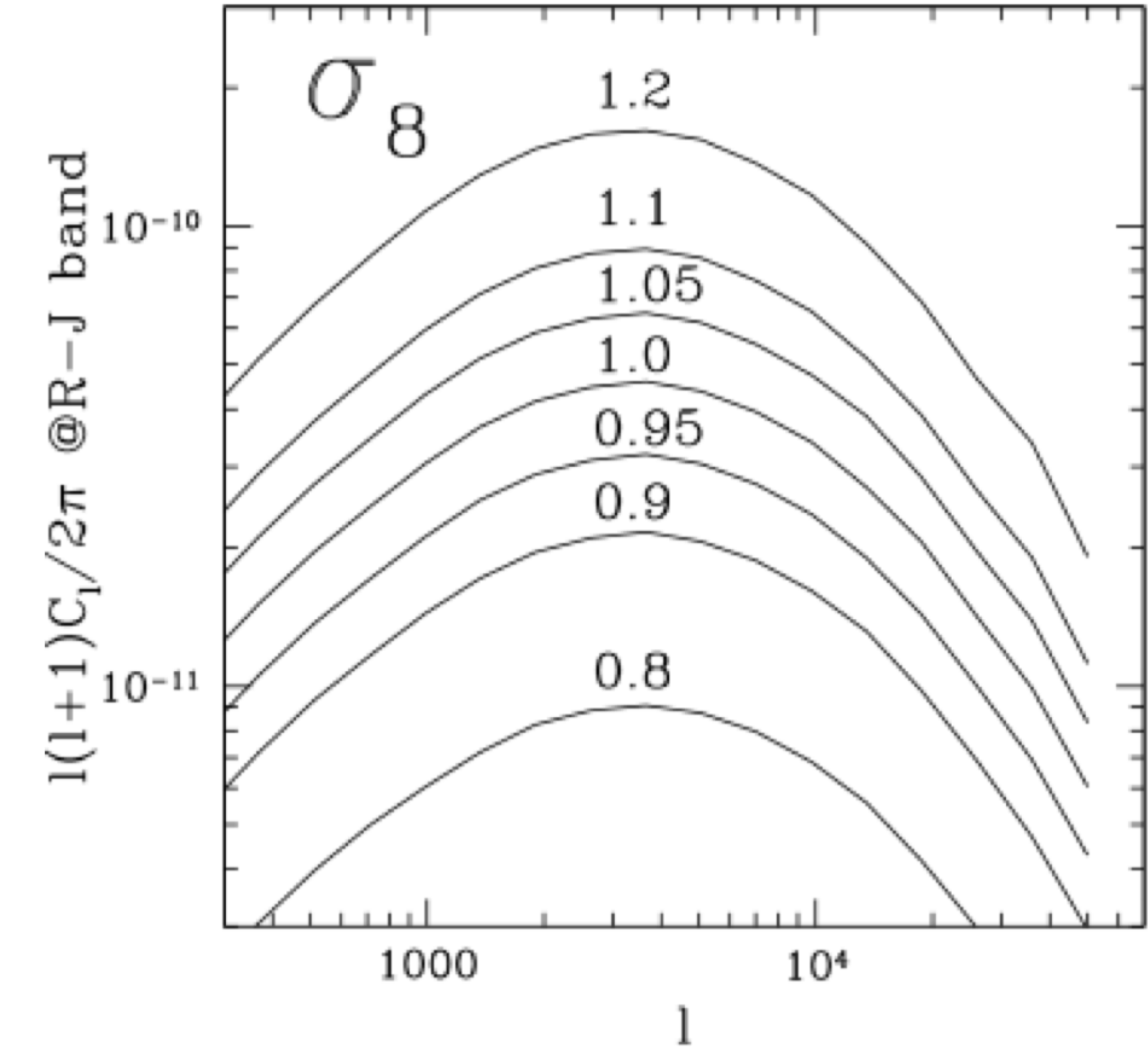


Source: Komatsu & Seljak (2002)

# tSZ Effect — Amplitude of matter fluctuations

Use  $\sigma_8$ , the mass dispersion on a scale of  $8h^{-1}\text{Mpc}$ , as a sphere of that radius contains an approximate amount of a cluster

As seen in the angular power spectrum of tSZ, there's also a strong dependence here



Source: Komatsu & Seljak (2002)

# tSZ Effect — ICM

- Focus shifted to ICM astrophysics when the main contribution to the tSZ power spectrum came from low-mass groups and clusters  
Also  $Y_{\text{SZ}}$  is proportional to thermal energy content of ICM
- Combine with X-ray measurements to constrain ICM astrophysics, especially
  1. Shock fronts: Shocks from cluster mergers heat the ICM, which should be observable in high spatial resolution tSZ measurements
  2. Pressure substructure: With high angular resolution imaging, tSZ is sensitive to this from the gas compression in merger events

# tSZ Effect — Extraction

- The method that yields the best S/N is through matched filters
- Based on approach described in Hasselfield et al. (2013), which uses the universal pressure profile developed by Arnaud et al. (2010)
- Pressure is modeled after generalized NFW profile, explicitly, electron pressure is

$$P(r) = P_{500} \left( \frac{M_{500}}{3 \times 10^{14} M_{\odot}} \right)^{\alpha_p} p(x)$$

where

$$P_{500} = 1.65 \times 10^{-3} E(z)^{8/3} \left( \frac{M_{500}}{3 \times 10^{14} M_{\odot}} \right) \text{keV cm}^{-3}$$

$$p(x) = P_0 (c_{500} x)^{-\gamma} (1 + (c_{500} x)^{\alpha})^{(\gamma - \beta)/\alpha}$$

# tSZ Effect — Extraction

- From this pressure profile and ignoring, relativistic effects, the Compton-y parameter becomes

$$P(r) = P_{500} \left( \frac{M_{500}}{3 \times 10^{14} M_\odot} \right)^{\alpha_p} p(x)$$

$$y(\theta) \propto \int ds P(\sqrt{s^2 + (R_{500}\theta/\theta_{500})^2})$$

where it is now a function of  $\theta$  and  $\theta_{500} = R_{500}/D_A(z)$

- When we combine the above expressions, quoting the result from Hasselfield et al. (2013), we find

$$y(\theta, m) \approx 10^{A_0} E(z)^2 m^{1+B_0} \tau(m^{C_0} \theta / \theta_{500})$$

to find the optical depth  $\tau$

# tSZ Effect — Extraction

- After finding the optical depth, a set of matched filters are created by first making signal templates based on the optical depth, i.e.  $S_{\theta_{500}}(\theta) \equiv \tau(\theta/\theta_{500})$
- The associated match filter is given by

$$\Psi_{\theta_{500}} = \frac{1}{\Sigma_{\theta_{500}}} \frac{B(\mathbf{k}) S_{\theta_{500}}(k)}{N(\mathbf{k})}$$

where

- $B(\mathbf{k})$  is the telescope beam response multiplied with the map pixel window function
- $N(\mathbf{k})$  is the anisotropic noise power spectrum of the map
- $\Sigma_{\theta_{500}}$  is a normalization factor

# kSZ Effect — Theory

- kSZ comes from scattering with electrons that move with large bulk velocities
- If the cluster velocity has a component along the line of sight to the cluster, see a distortion in the CMB
- This distortion, in the non-relativistic limit is given in SZ (1980)

$$\frac{\Delta T_{kSZ}}{T_{CMB}} = - \int d\ell \sigma_T n_e \frac{\mathbf{v}_{pec} \cdot \hat{r}}{c} = -\tau_e \left( \frac{v_{pec}}{c} \right)$$

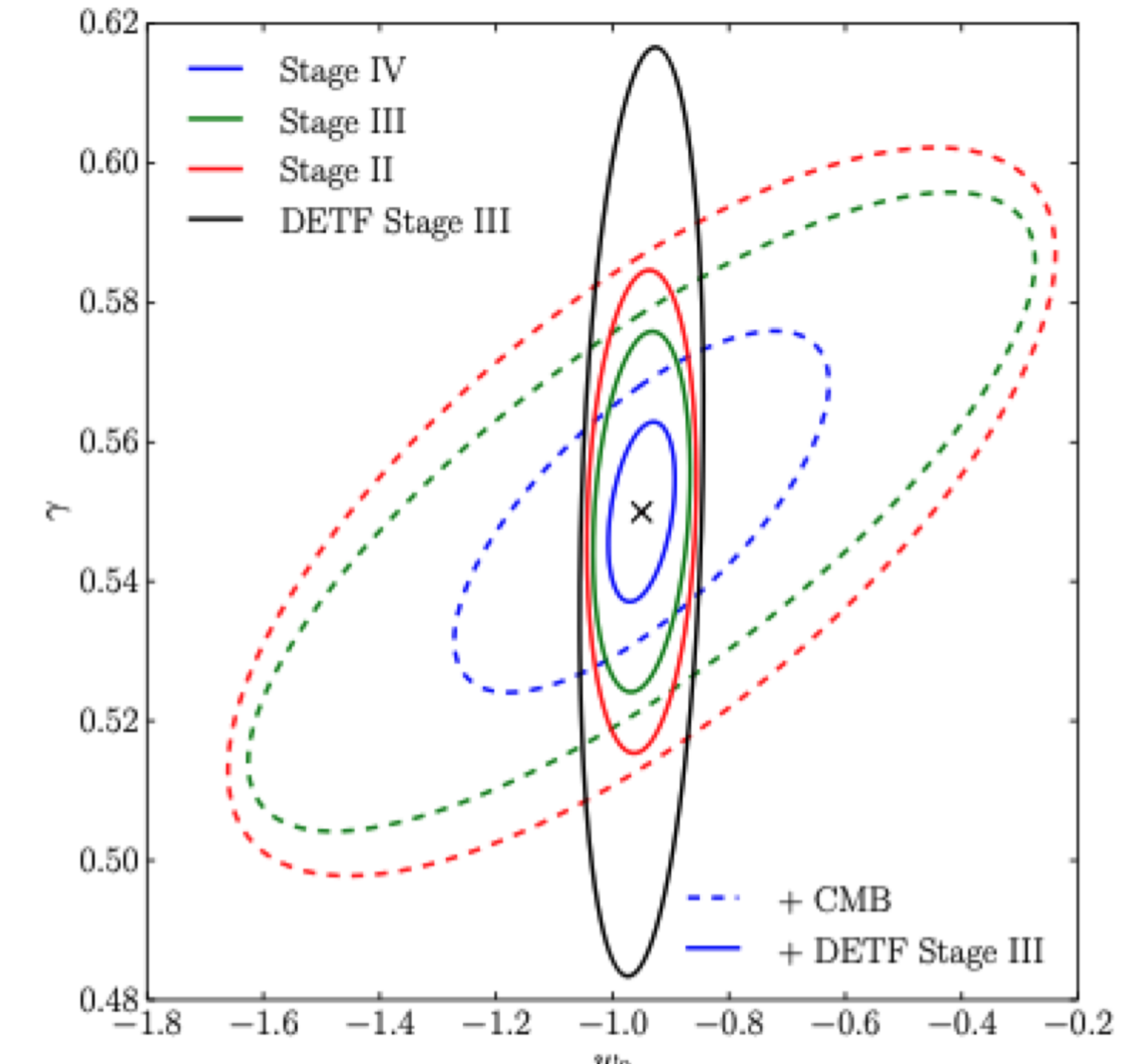
where  $\mathbf{v}_{pec}$  is along the line of sight

# kSZ Effect — Applications

- On small enough scales, mutual gravitational attraction causes clusters of galaxies to move towards each other
- Therefore, a measurement of this pairwise motion can be a valuable consistency check for the standard cosmological model
- average velocity at which clusters at a given distance move towards each other (pairwise velocity of clusters) can be estimated using only information about their LOS velocities, but practically difficult to measure
- Relationship between  $v_{\text{pec}}$  and kSZ signal can be a potential probe to these LOS velocities

# kSZ Effect — Cosmological Models

- Mueller et al. (2015) have shown that the mean pairwise velocity,  $V$ , is particularly sensitive to the growth of structure,  $\gamma$ , and  $w_0$ , the present-day value of the dark energy equation of state
- The uncertainties shown on the left are calculated, via the Fisher matrix formalism (will go over next)
- Provide an alternative and independent probe of gravity's influence on cosmic structure



Source: Mueller et al. (2015)

# Aside — Fisher matrix formalism with a toy model

- Based on Wittman's treatment of Fisher matrices for beginners  
Consider a case where we have two observables,  $n_1$  and  $n_2$ , which each have measurement uncertainty,  $\sigma_1$  and  $\sigma_2$
- Furthermore, we only have two model parameters, pair production rate,  $\alpha$  and 2-production only rate ( $\beta$ ), so the model reads us

$$n_1 = \alpha + \beta$$

$$n_2 = \alpha$$

- If we over/under-estimate our measurements, there will be a nonzero covariance between our estimates of the two parameters, how to get this covariance

# Aside — Fisher matrix formalism with a toy model

- This is where Fisher matrices come into play because you just need to know your model and your measurement uncertainties to find these covariances
- Because the inverse of the Fisher matrix, is the covariance matrix, which in turn places constraints on the uncertainty of our model parameters, since the Fisher matrix is the ‘best possible’ we can do given the content from the experiment
- Generally, for N model parameters,  $p_1, p_2, \dots, p_N$ , the Fisher matrix  $F$  is an  $N \times N$  symmetric matrix, and assuming we have B observables,  $f_1, f_2, \dots, f_B$ , then the elements of the Fisher matrix are

$$F_{jk} = \sum_b \frac{1}{\sigma_b^2} \frac{\partial f_b}{\partial p_j} \frac{\partial f_b}{\partial p_k}$$

## Aside — Fisher matrix formalism with a toy model

- Going back to our toy model, the Fisher matrix reads

$$F = \begin{pmatrix} \frac{1}{\sigma_1^2} + \frac{1}{\sigma_2^2} & \frac{1}{\sigma_1^2} \\ \frac{1}{\sigma_1^2} & \frac{1}{\sigma_1^2} \end{pmatrix}$$

$$\begin{aligned} n_1 &= \alpha + \beta \\ n_2 &= \alpha \end{aligned}$$

$$F_{jk} = \sum_b \frac{1}{\sigma_b^2} \frac{\partial f_b}{\partial p_j} \frac{\partial f_b}{\partial p_k}$$

where the covariance is calculated from taking the inverse

$$\begin{pmatrix} \sigma_2^2 & -\sigma_2^2 \\ -\sigma_2^2 & \sigma_1^2 + \sigma_2^2 \end{pmatrix}$$

can expand this to arbitrary amounts of parameters and observables, but at that point, would be better to do so computationally.

# Aside — Fisher matrix formalism with a toy model

- Other practical aspects of Fisher matrices include:
  1. Assuming Gaussian priors with width  $\sigma$ ; we can just add it to the appropriate diagonal element of Fisher matrix
  2. If we want a Fisher matrix for a smaller parameter space, we can marginalize over nuisance parameters, with the following steps: invert  $F$ , then remove rows and columns marginalized over, then invert  $F$  again.
  3. If we have 2 independent data sets A and B, the Fisher matrix for the combined distribution is simply adding the two respective Fisher matrices

# kSZ Effect — Other applications

- *Massive neutrinos*: extending the  $\Lambda$ CDM parameter space to include massive neutrinos, can constrain similarly as the growth of structure, the masses of neutrinos (Mueller et al. (2015))
- *ICM substructure*: maps of kSZ signal can measure internal gas motions in the ICM (Nagai et al., 2003)
- *Missing baryons*: A cosmic web, which cannot be detected by AGN and X-ray measurements, of filaments should be found at temperatures  $10^5 - 10^7$  K; Both tSZ and kSZ traces distribution of baryons, some of which could be in the cosmic web (Cen & Ostriker, 2006)
- *Reionization*: Left imprints on the CMB, which can be observed in the kSZ power spectrum (Battaglia et al. (2013)).

# kSZ Effect — Extraction

- Signal for single clusters have a small amplitude ( $\sim \mu\text{K}$ ) and degenerate spectral dependence with the CMB, more practical to measure pairwise motion of the clusters
- There are multiple ways to extract this signal, expand on the Aperture Photometry (AP) method as done in Calafut et al. (2017).
- Assumes that the kSZ is localized in the cluster and that the CMB is correlated over long wavelengths  
When we take the difference, we remove the CMB contribution, while keeping the kSZ signal intact

# kSZ Effect — Extraction

- Specifically, the AP temperature is the difference between the average CMB pixel temperature within a given angular radius  $\Theta$ , and CMB pixel temperature within an annulus outside the radius of width  $\text{Sqrt}(2\Theta)$ , i.e.  $T_{AP} = \langle T_{inner} \rangle - \langle T_{annul} \rangle$ .
- The kSZ temperature decrement is then given by  $\Delta T_i = T_{AP} - \bar{T}_{AP}$  where the first term is the kSZ amplitude from AP, and the second term is averaged aperture temperature over all cluster locations as done in Hand et al. (2012), given by

$$\bar{T}_{AP} = \frac{\sum_j T_{AP} \exp\left(-\frac{(z_i - z_j)^2}{2\sigma_z^2}\right)}{\sum_j \exp\left(-\frac{(z_i - z_j)^2}{2\sigma_z^2}\right)}$$

# kSZ Effect — Extraction

- The peculiar velocity correlations are then found by using the pairwise kSZ signal estimator described in Hand et al. (2012),

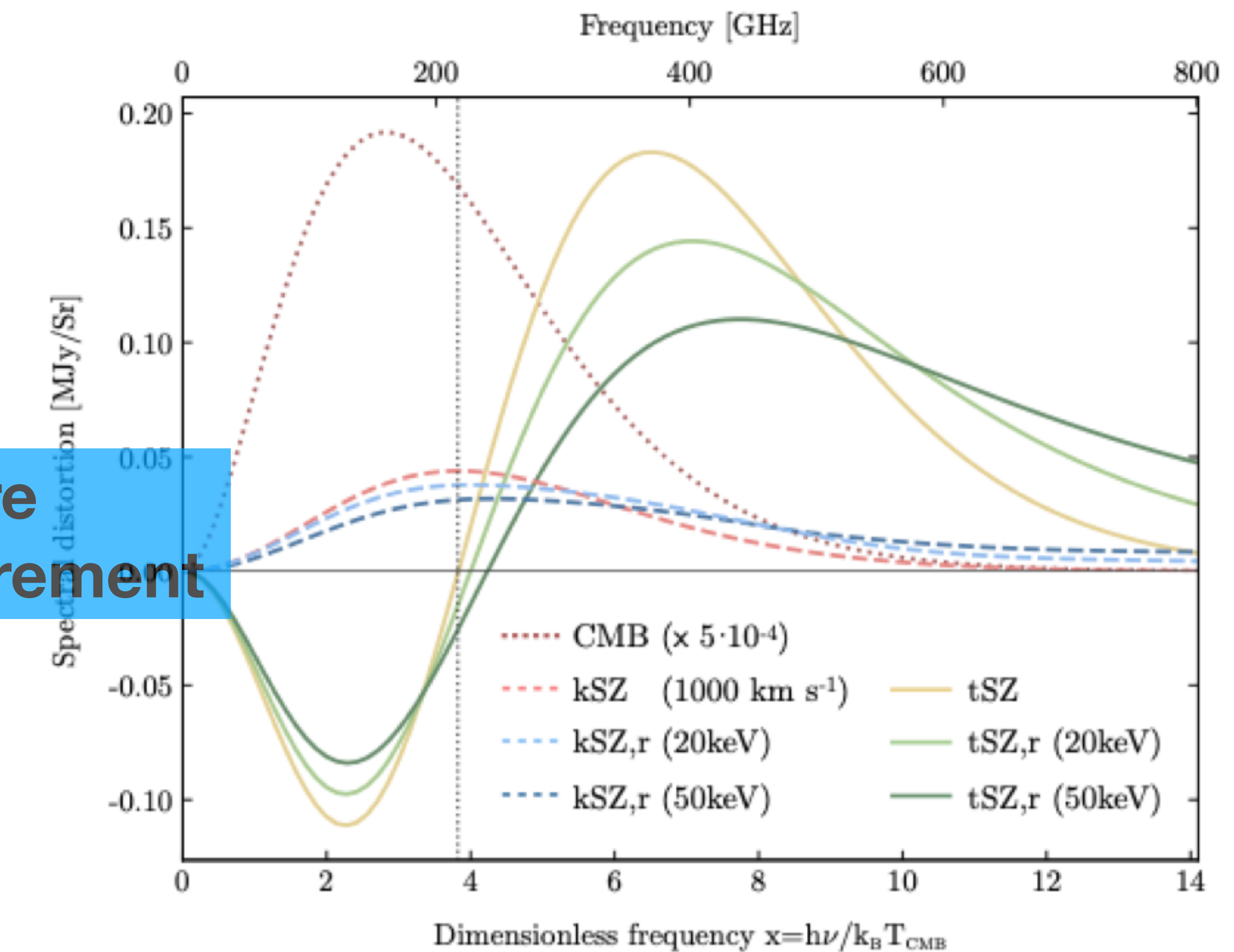
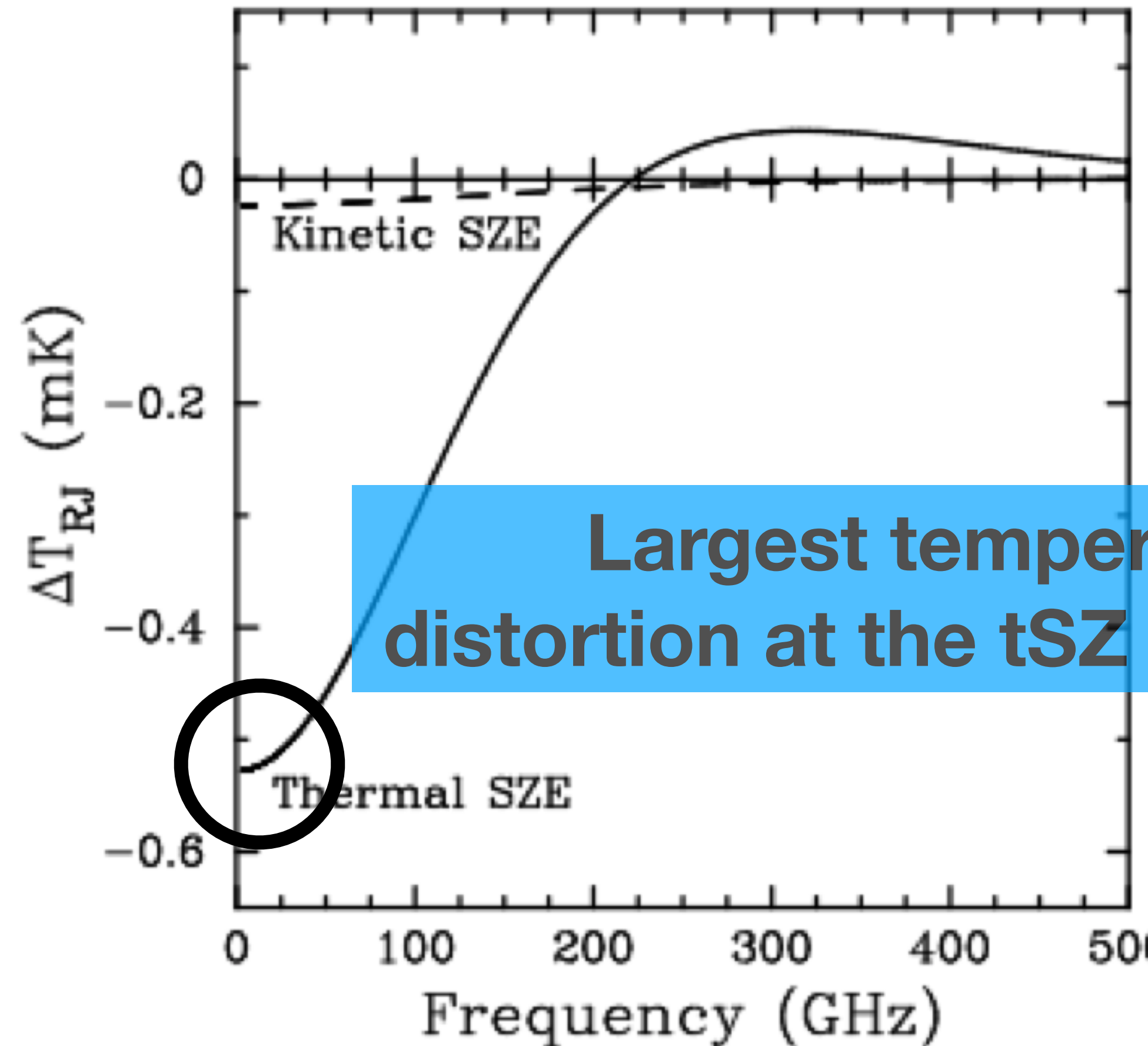
$$\hat{p}_{kSZ}(r) = -\frac{\sum_{i < j} (\Delta T_i - \Delta T_k) c_{ij}}{\sum_{i < j} c_{ij}^2}$$

where the sum is over all cluster pairs and the weights are calculated with

$$c_{ij} = \hat{r}_{ij} \cdot \frac{\hat{r}_i + \hat{r}_j}{2} = \frac{(r_i - r_j)(1 + \cos \alpha)}{2\sqrt{r_i^2 + r_j^2 - 2r_i r_j \cos \alpha}}$$

- There are also other approaches include cross-correlation of the CMB map with a velocity field, which has been constructed from the position of galaxies with linear perturbation theory (velocity reconstruction Schaan et al., 2015), and using the square of CMB anisotropy maps (projected fields, Ferraro et al., 2016)

# Previous Observations — tSZ History



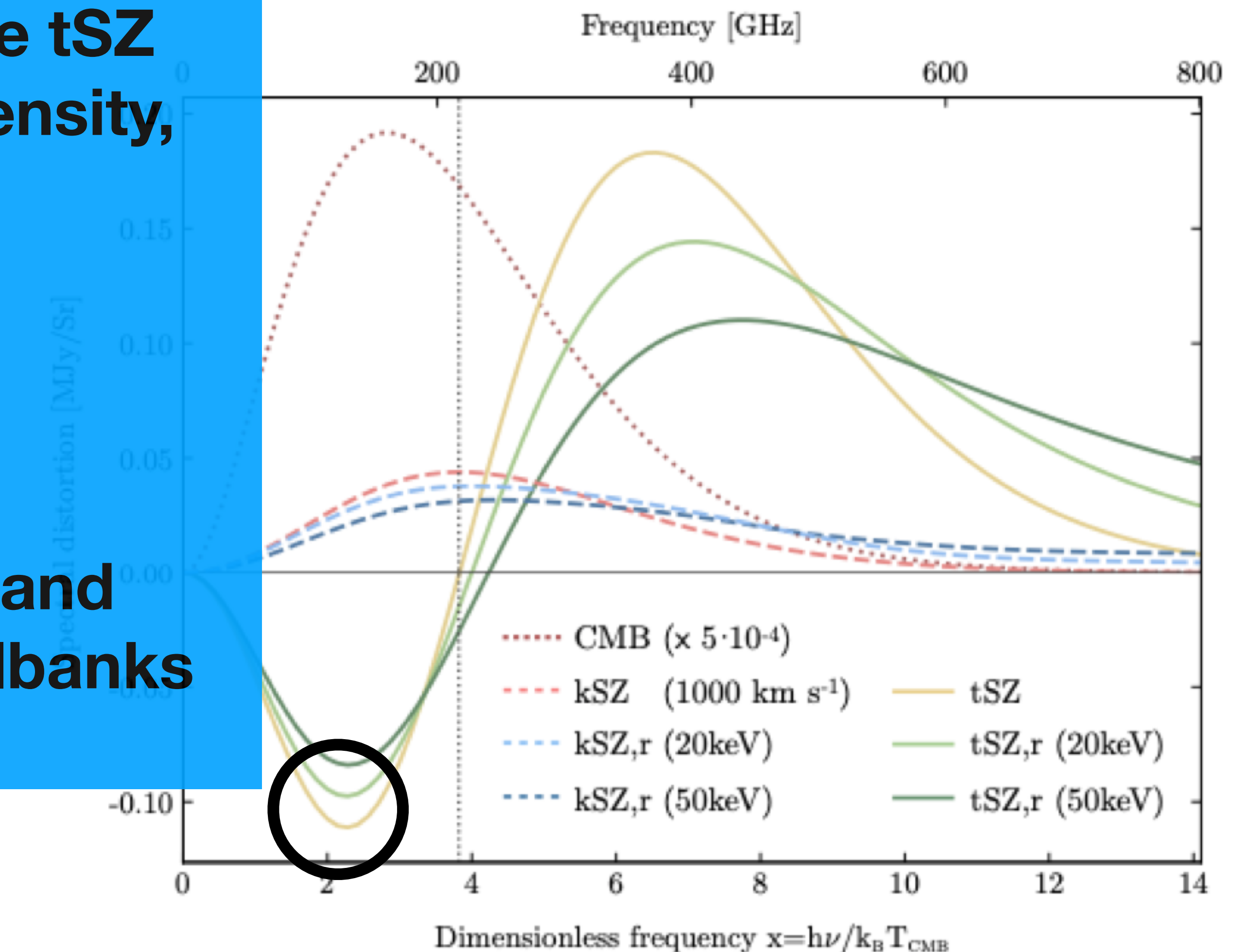
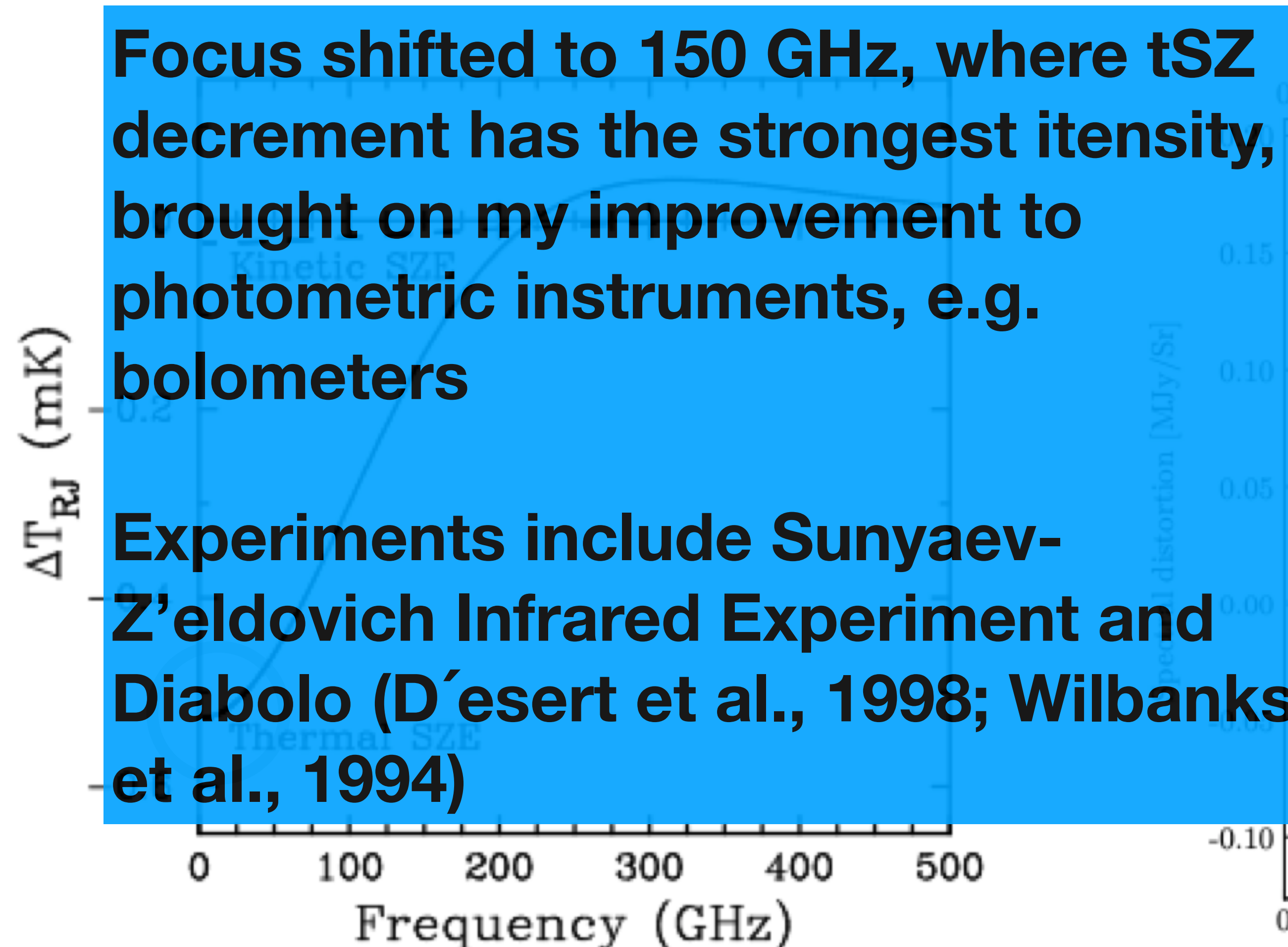
# Previous Observations — tSZ History

Birkinshaw et al., 1978 and Gull & Northover, 1976 used the Chilbolton Observatory (below) to probe the decrement, by focusing at 15 GHz

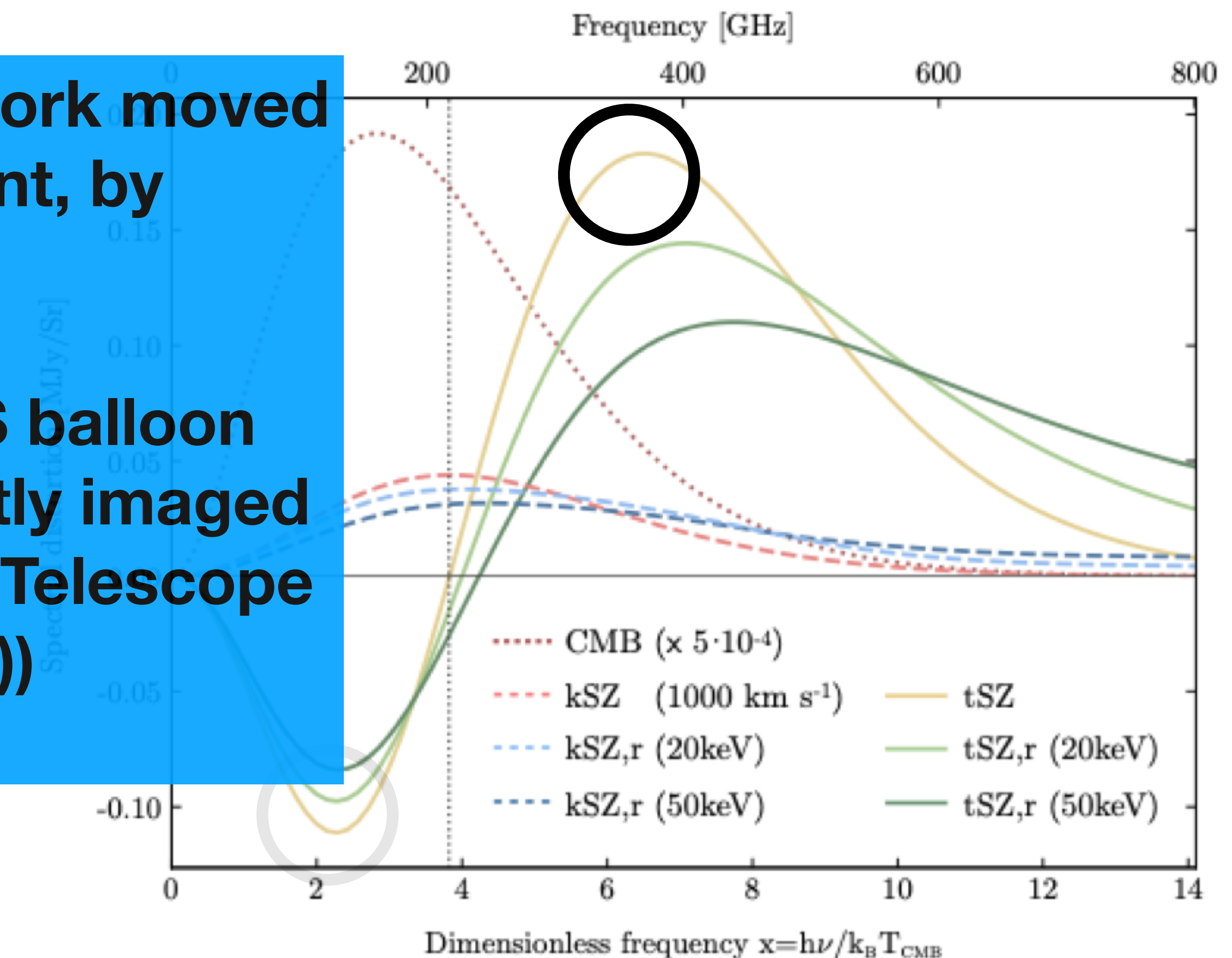
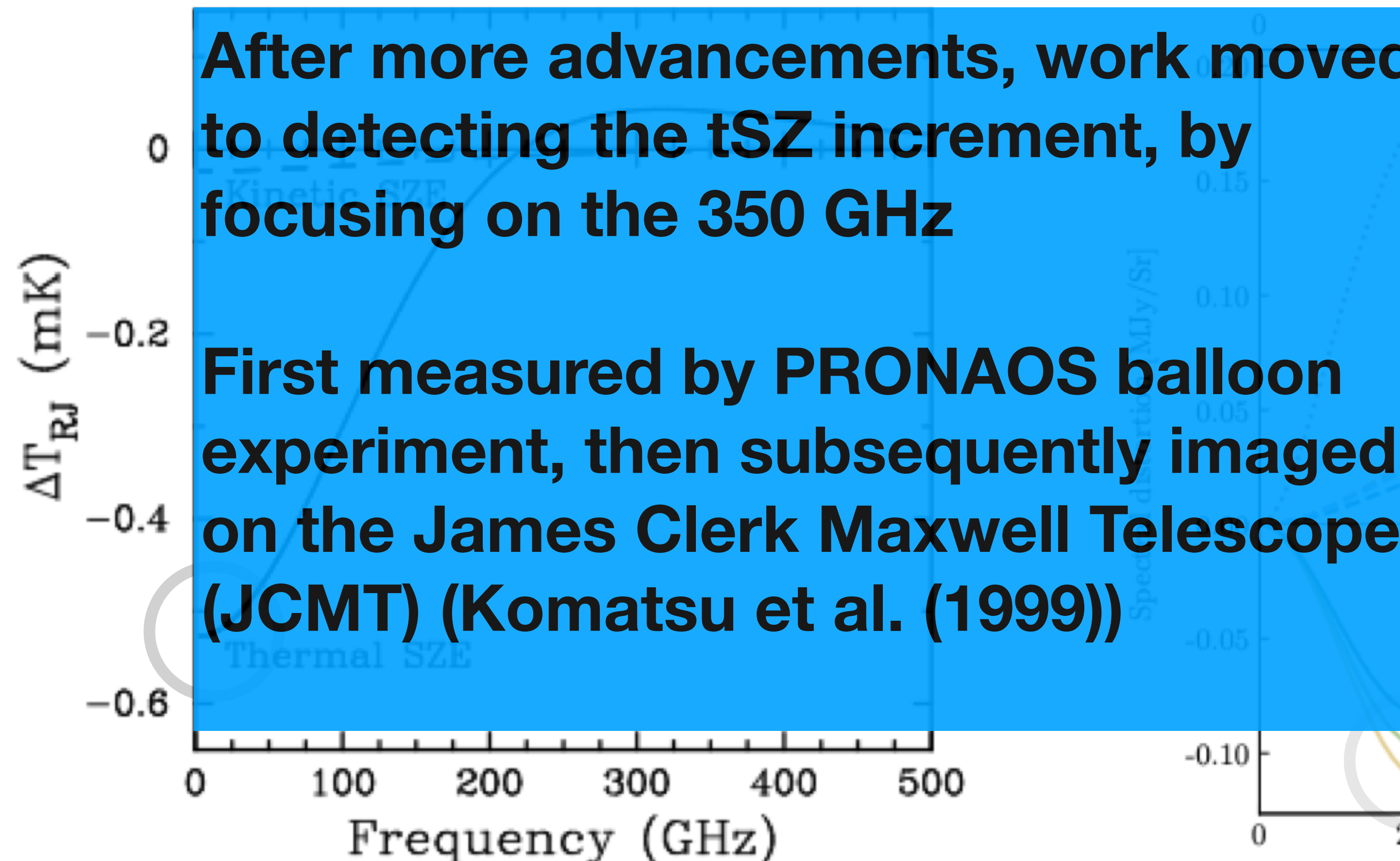


More reliable detections were made at the Owens Valley Radio Observatory (OVRO) 40-meter (above) by Birkinshaw et al., 1984

# Previous Observations — tSZ History



# Previous Observations — tSZ History

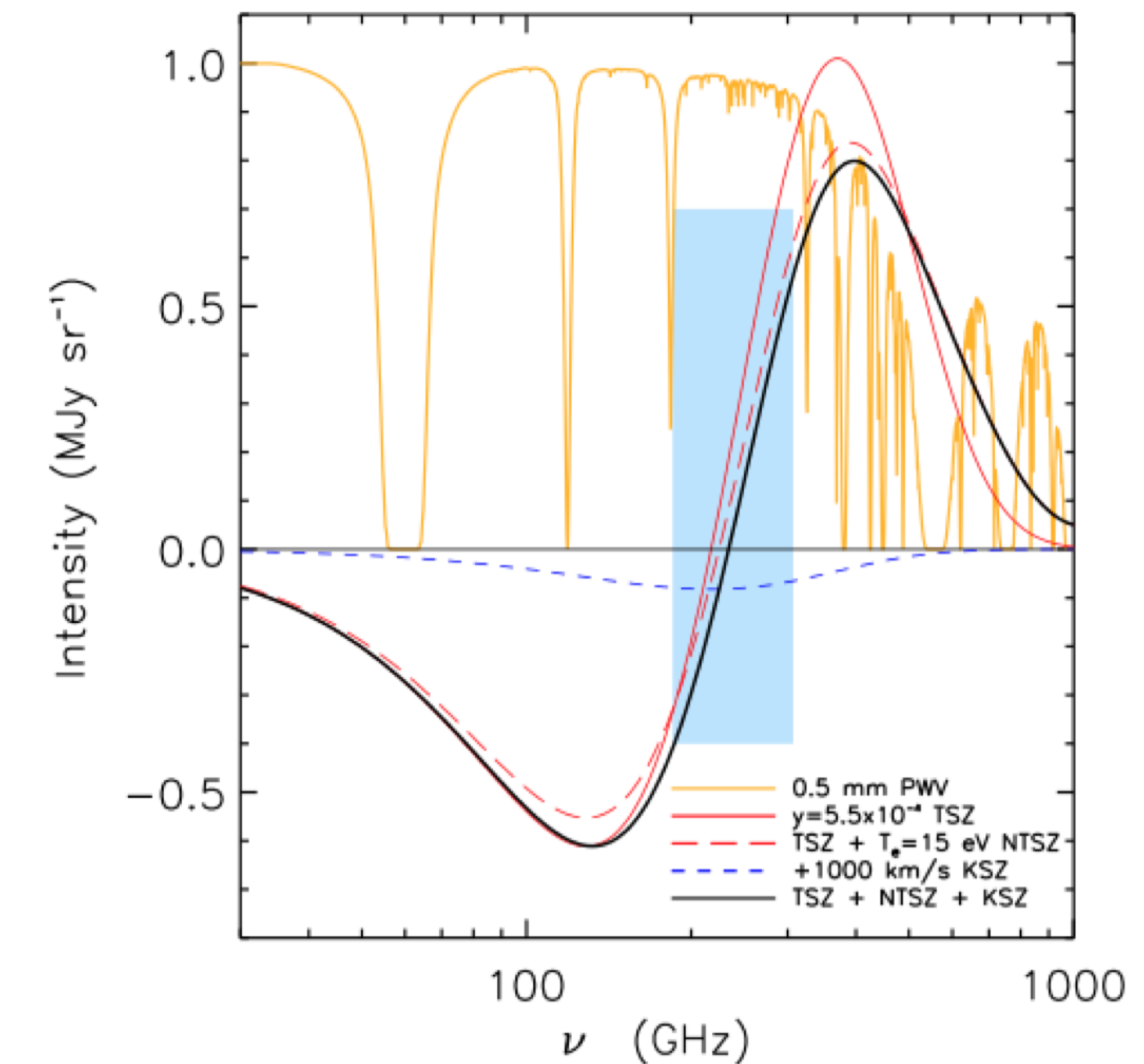


# Previous Observations — tSZ History

Having this information, the next step is to study the entire spectrum

First high resolution image (right), came from the Z-spec (Zemcov et al. 2012)

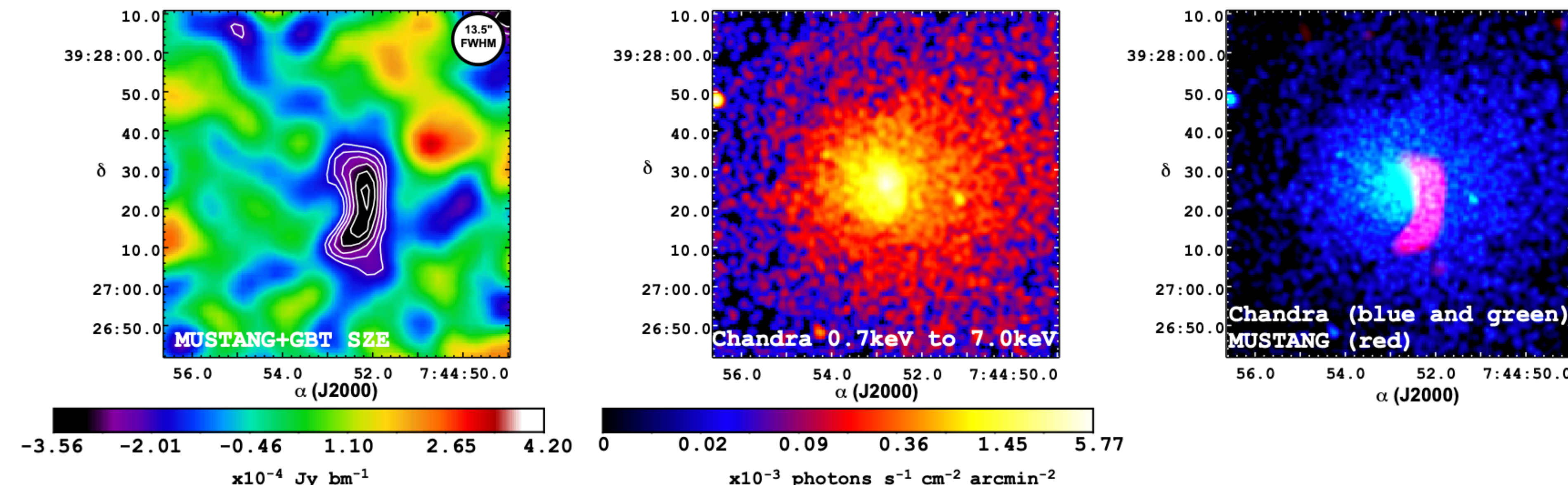
Done by focusing towards the cluster RX J1347.5-1145



# Previous Observations — tSZ History

Another significant improvement. came in the angular resolution with the use of the Multiplexed SQUID/TEC Array at Ninety Gigahertz (MUSTANG) Camera on the 100-m Green Bank Telescope (GBT)

Allowed for tSZ measurements from shocks (below) and pressure substructures in handful of clusters (Dicker et al., 2008; Korngut et al., 2011)



Source: Korngut et al. (2011)

# Previous Observations — tSZ History

- Have focused on single dish telescopes so far.  
Now, make an array of them, can then combine these signals, essentially making a larger antenna and improving the resolution, without having to build large aperture elements, i.e. interferometers
- Comes at the expense of less sensitivity and slower mapping speeds



First interferometric measurements performed at the Very Large Array (shown left) and the Ryle telescope

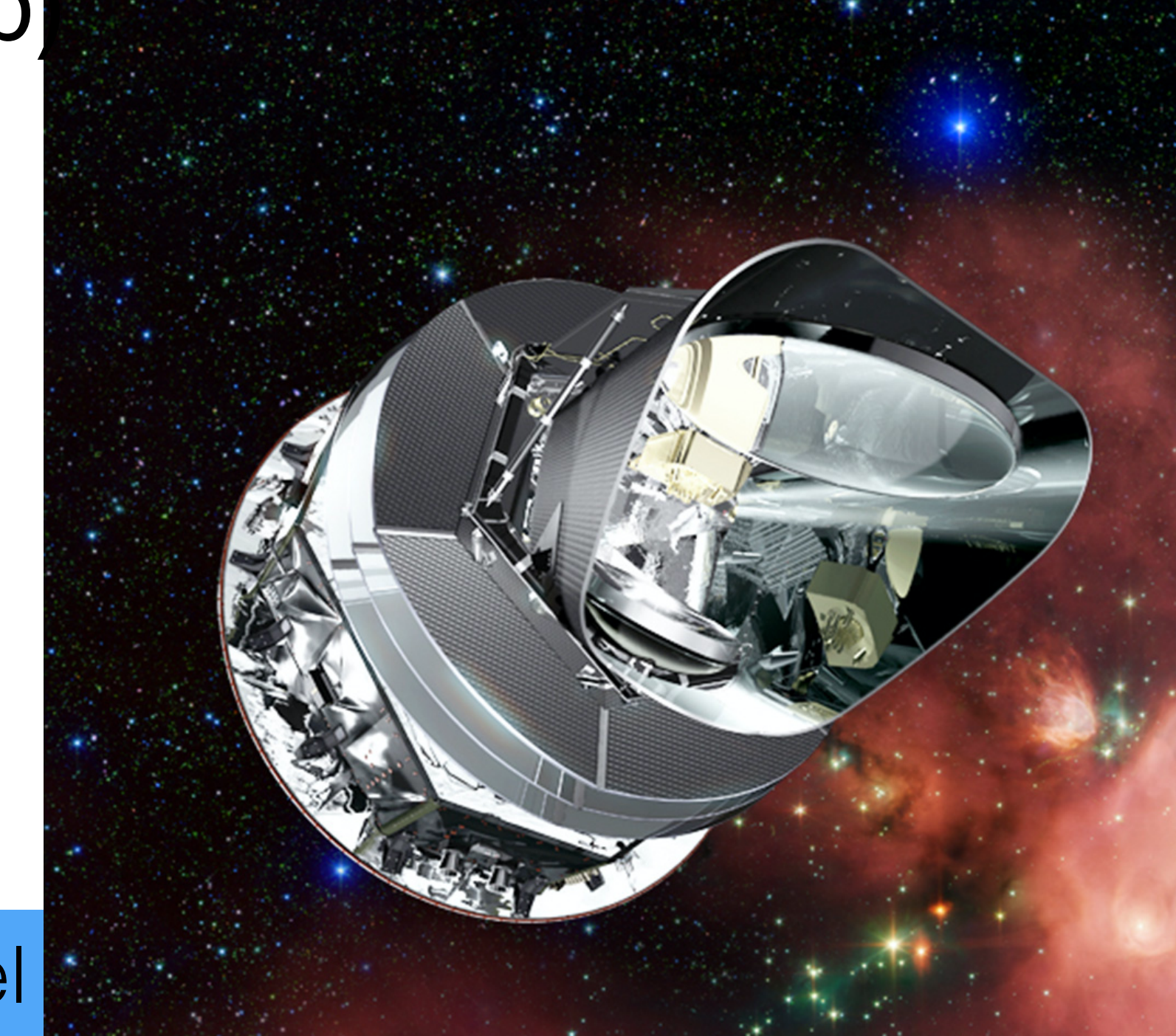
Provided first imaging and detection of the tSZ decrement just based on the signal  
(Moffet & Birkinshaw, 1989 & Jones et al., 1993)

# Previous Observations — tSZ History

- Focus then moved on to make maps/surveys of the SZ signal to allow for the study of the growth of structure as well as have probes of cosmology
- IRAM 30-m telescope and the NRO 45-m telescope delivered a  $5' \times 5'$  and  $2' \times 2'$  map, with  $20''$  and  $13''$  resolution, respectively (Komatsu et al., 1999, 2001), which exhibited an excess in SZ signal
- Improvements in photometric imaging arrays, such as at the Atacama Pathfinder Experiment Sunyaev-Zeldovich Experiment (APEX-SZ) and the Array for Microwave Background Anisotropy (AMiBA) imaged large statistical samples (Schwan et al., 2003 and Muchovej et al. 2007)

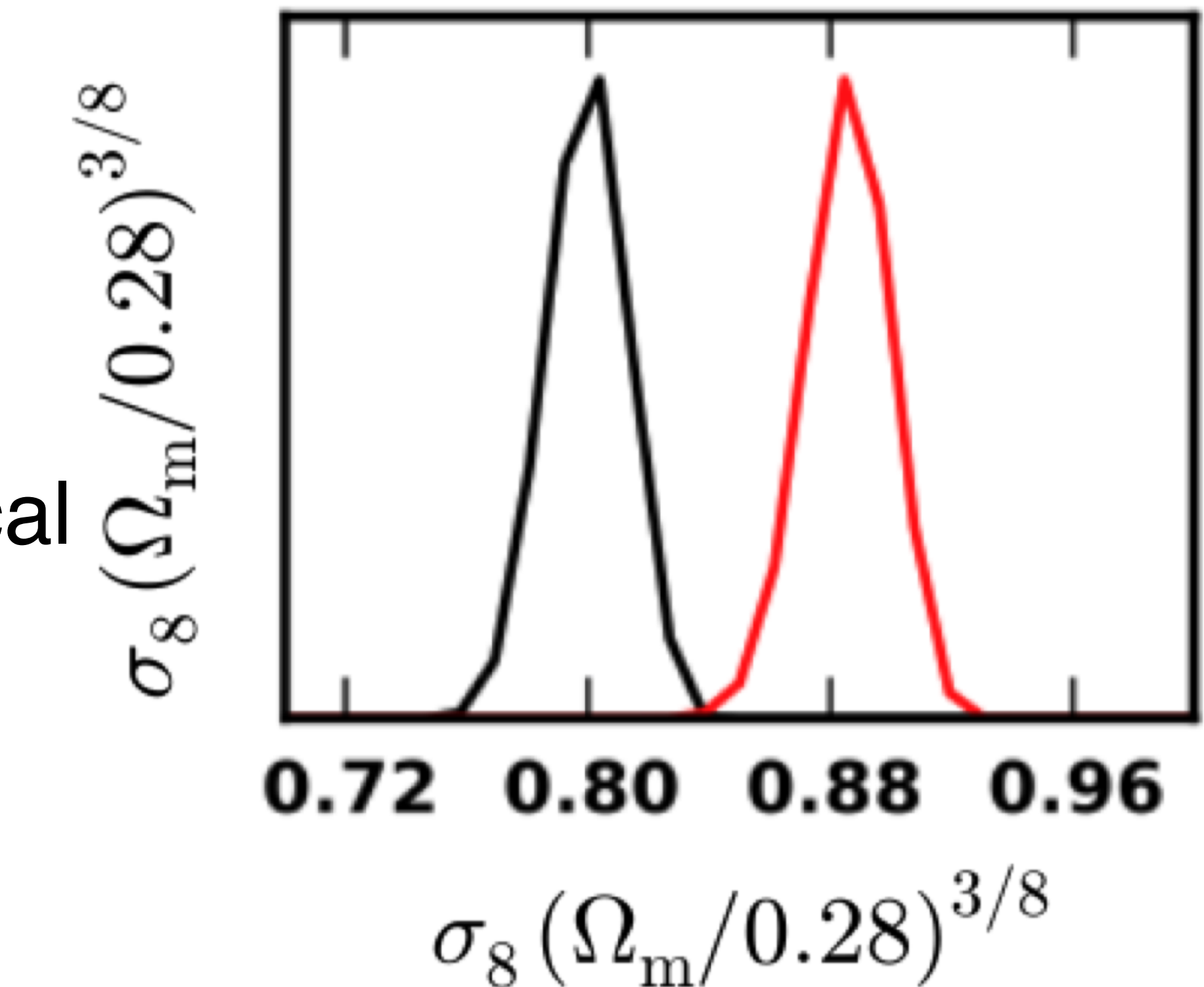
# Previous Observations — tSZ History

- Around a decade ago, the South Pole Telescope (SPT) and the Atacama Cosmology Telescope (ACT) (bottom left), achieved high mapping speeds to allow for wide-field surveys based on their tSZ signals (Menanteau et al., 2010; Staniszewski et al., 2009)
- Complemented by the Planck satellite (bottom right), which delivered a catalogue of roughly 2000 SZ clusters (Ade et al., 2016b)



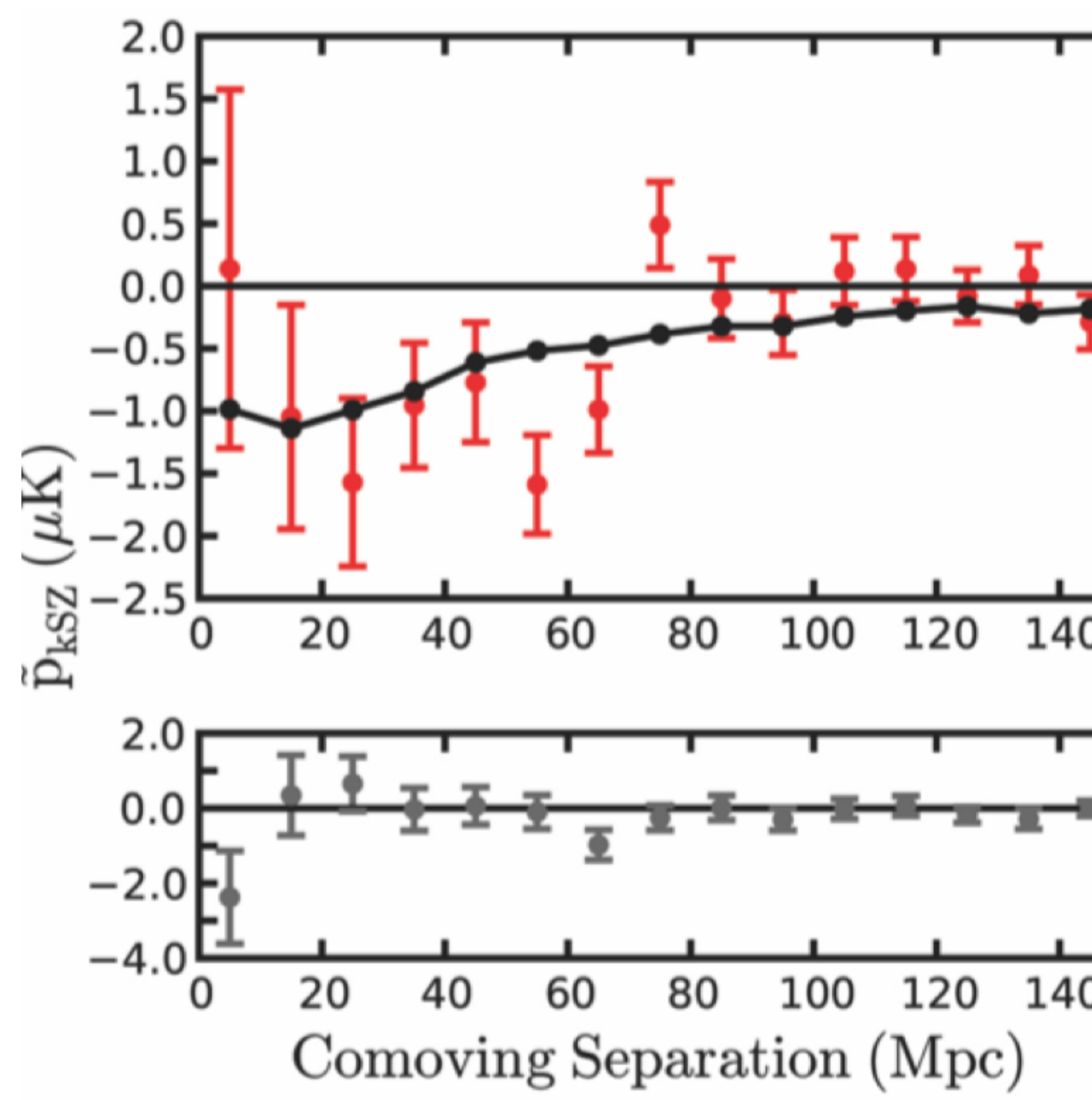
# Previous Observations — tSZ History

- Because of the photometric bands that spanned, 30-850 GHz, Planck data gave the broadest frequency coverage of the tSZ spectrum to date (Hurier, 2016)
- Planck tSZ data placed constraints on cosmological parameters, like  $\sigma_8$  (right)
- Shocks were also studied near the Coma Cluster (Ade et al., 2013)
- Provided first detection of the cosmic web, recovering a significant portion of the missing baryons (Tanimura et al., 2019)



Source: Aghanim et al. (2016).

# Previous Observations — kSZ History



Hand et al. (2012) combined CMB data from ACT and the Baryon Oscillation Spectroscopic Survey (BOSS) spectroscopic catalog (Ahn et al., 2012)

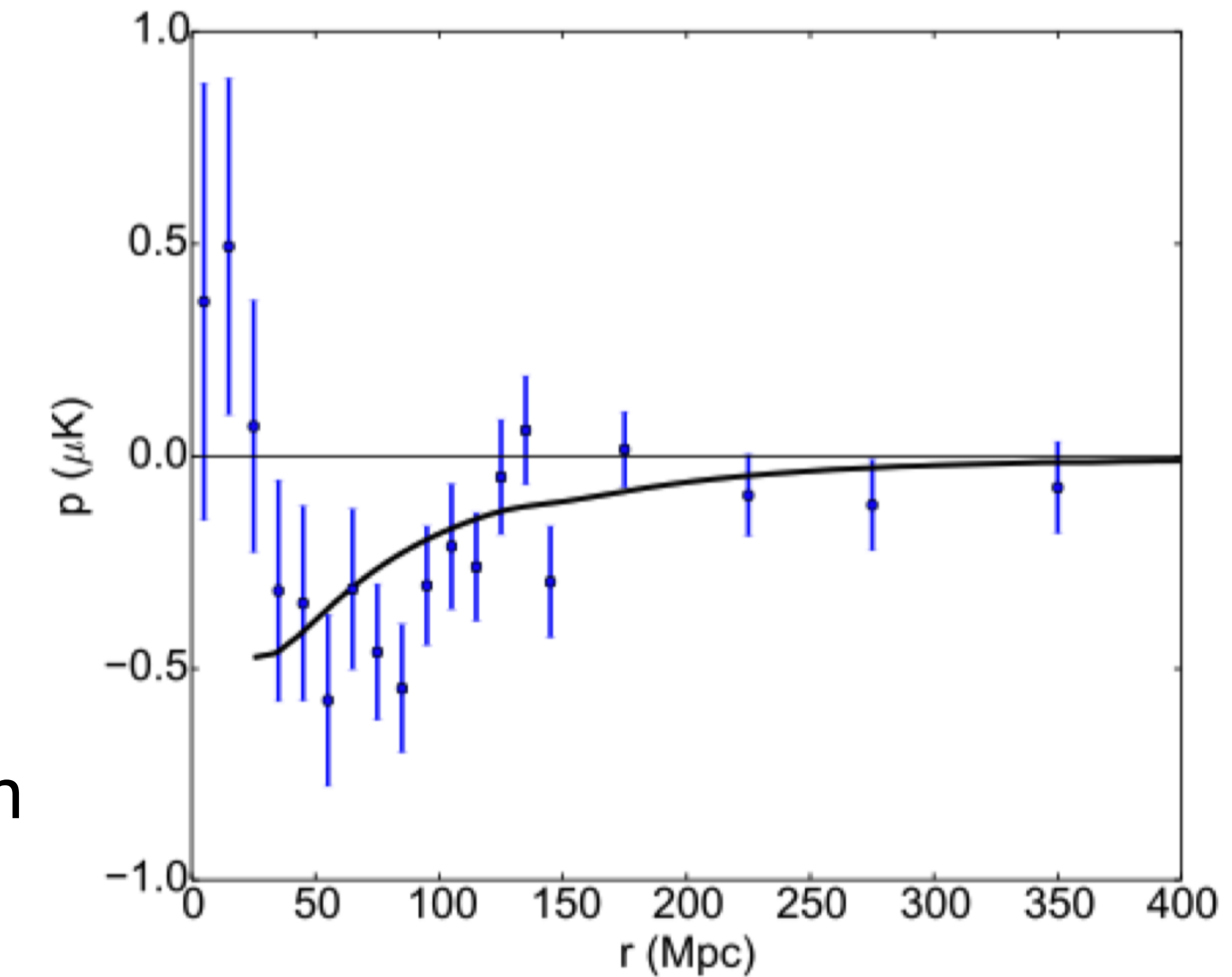
First pairwise kSZ signal from the analysis, shown on left

Subsequent detections were found in Planck CMB data with the Central Galaxy Catalog from the Sloan Digital Sky Survey (SDSS) with a statistical significance of  $1.8 - 2.5\sigma$

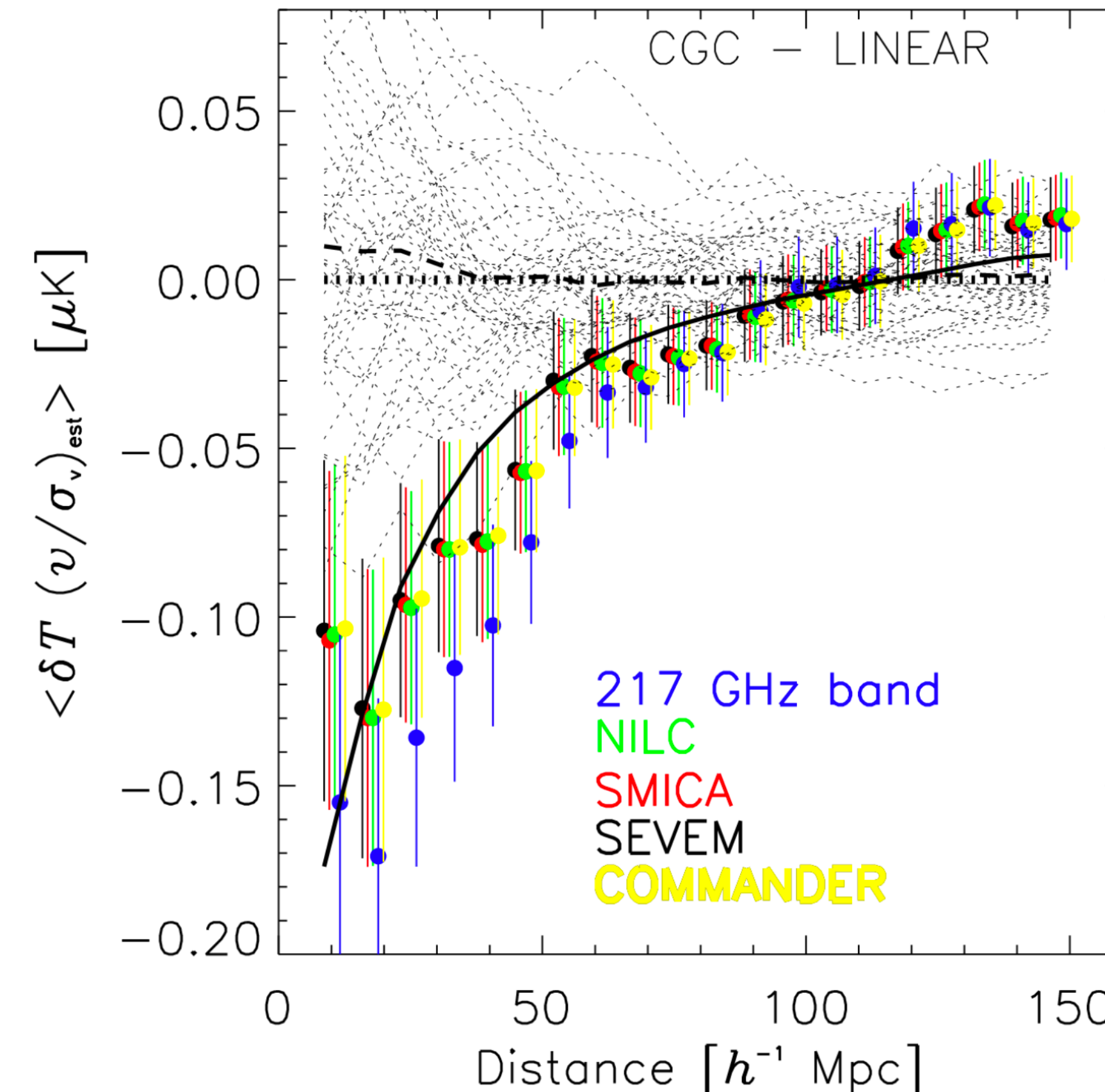
# Previous Observations — kSZ History

The pairwise kSZ signal was found by combining SPT CMB data with the galaxy cluster catalog from the Dark Energy Survey, reporting a  $4.2\sigma$  significance (Soergel et al. (2016))

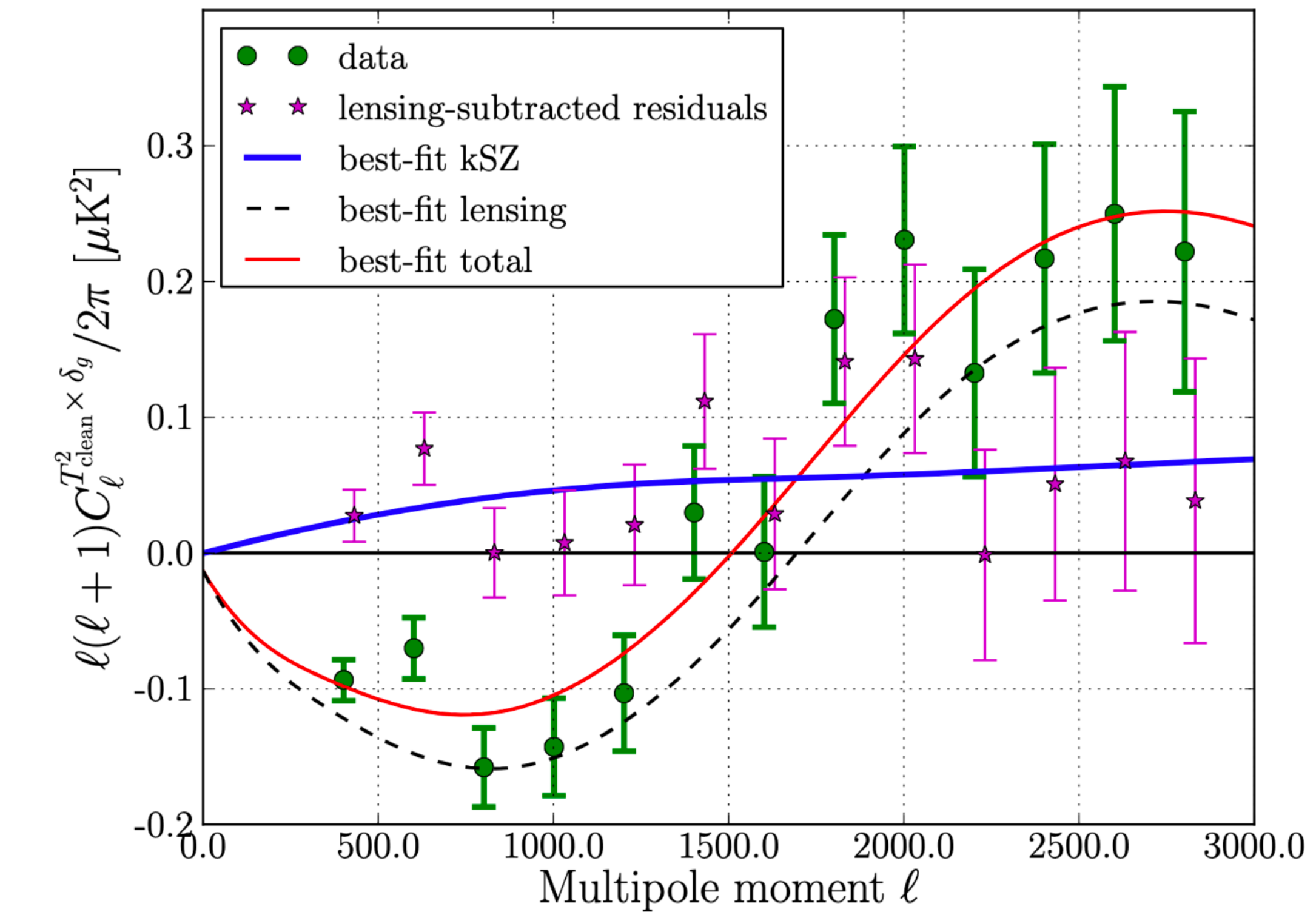
Expanded on by Bernardis et al. (2017) by combining ACTPol data with the BOSS DR11 data, with a  $4.1\sigma$  significance, shown on the right



# Previous Observations — kSZ History



kSZ from velocity reconstruction  
from Planck, with  $3.0 - 3.7\sigma$   
significance (Ade et al. 2016)



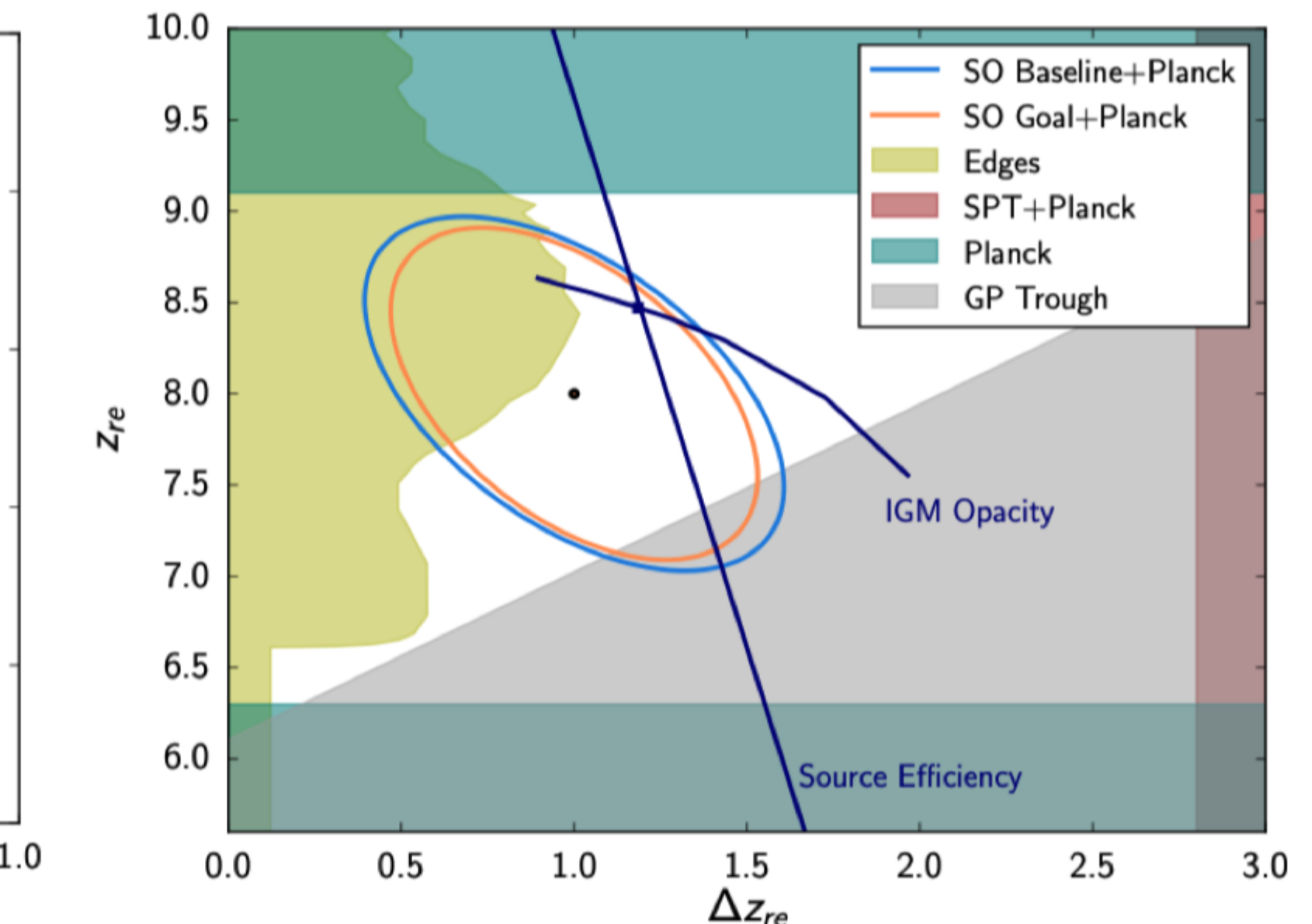
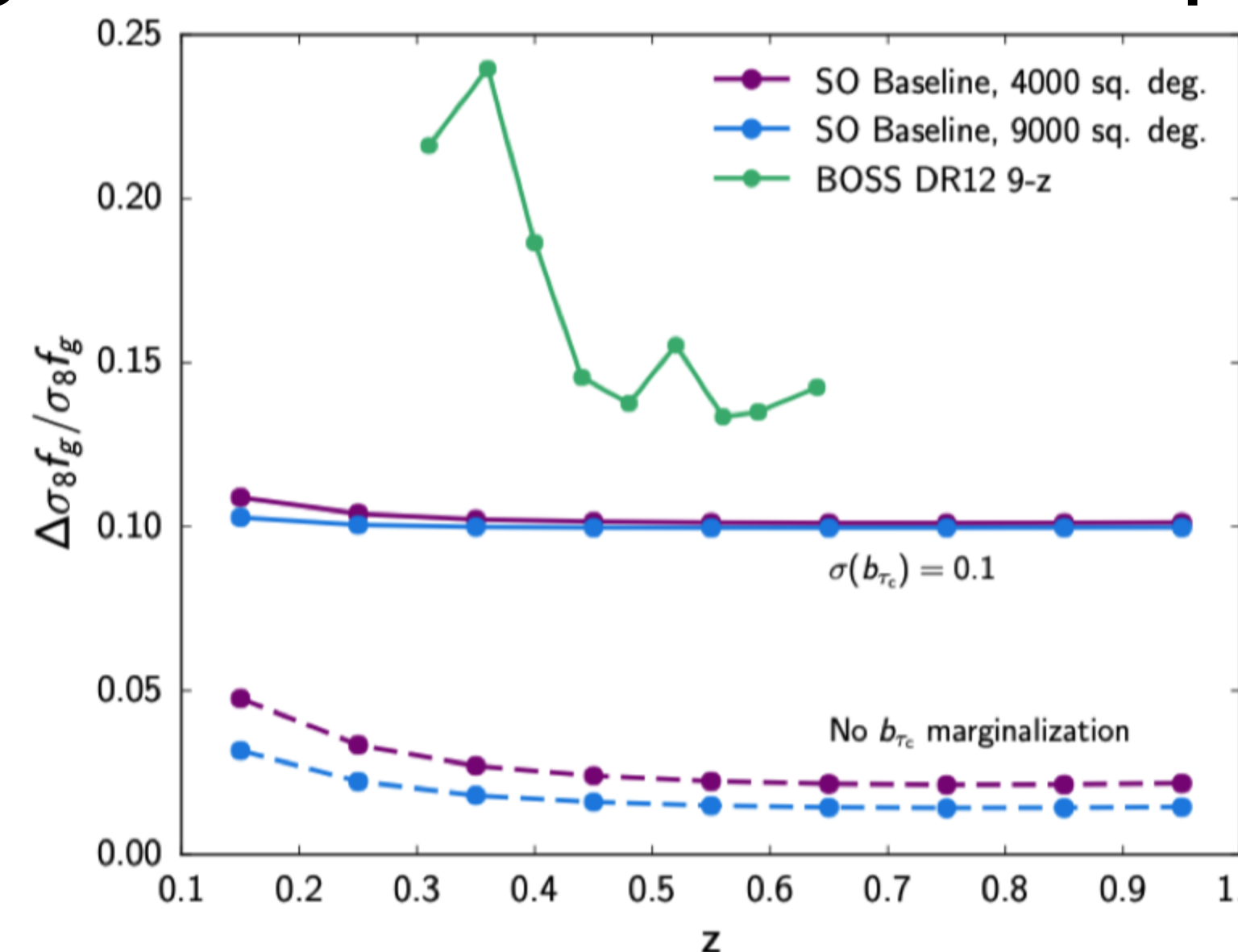
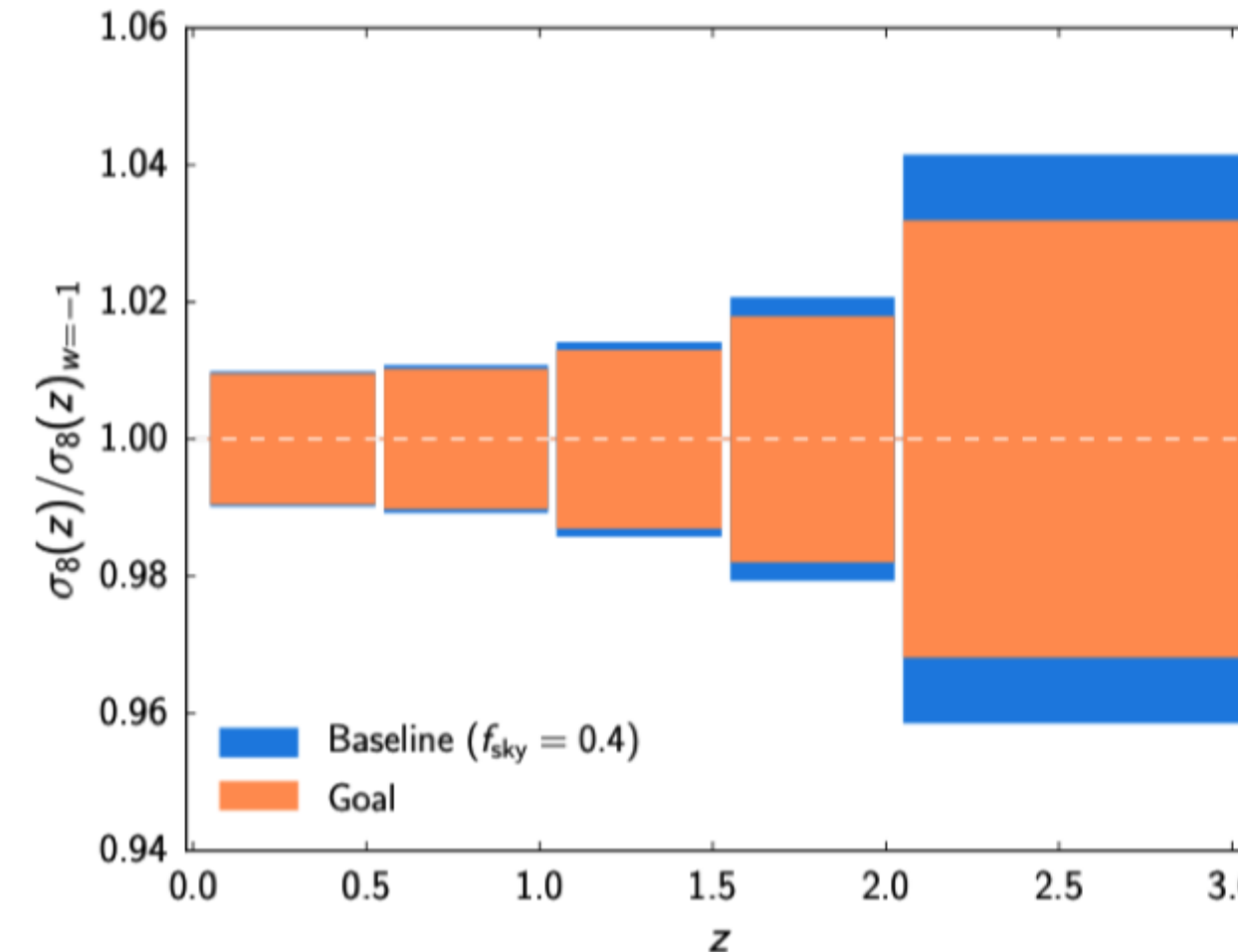
kSZ power spectrum from projected  
field estimator from  
Planck+WMAP+WISE, with  $3.8 - 4.5\sigma$  significance (Hill et al. 2016)

# Current Experiments

- Upgrades to the Atacama Large Millimeter/Submillimeter Array (**ALMA**) in the next few years include 2 bands covering 35 – 90 GHz, which are frequencies best suited for probing the tSZ; Kitayama et al. (2016) showed that it can have up to 5" resolution
- 2nd generation MUSTANG (**MUSTANG-2**) will replace MUSTANG-1 on the GBT; one of the highest resolution bolometer cameras to probe the tSZ at 9" resolution (Dicker et al., 2014)
- New IRAM Kid Arrays 2 (**NIKA2**) operating at 150 mK (Adam et al., 2018) boasts a dual band camera, 260 GHz map to detect point sources, and high angular resolution and FOV

# Future Experiments — Simons Observatory (SO)

- Combine various experiments at the Atacama Desert (Ade et al., 2019)
- SO aims to deliver strong constraints on the kSZ effect, as well as the ability to separate SZ components from each other, and should have first light in 2021
- Various forecasts, which were calculated using Fisher matrices, are shown below, including  $\sigma_8$ , logarithmic growth rate of LSS, and epoch of reionization



# Future Experiments

- For **CMB-S4**, the tSZ here will most likely be extracted from abundance of clustering of galaxy clusters, while for kSZ, it's not yet clear (Azabajian et al. 2016), while an anticipated start date is in 2028, it should have couple orders of magnitude more detectors than SO
- The Large Millimeter Wave Telescope (LMT) 50 m at Sierra Negra, Mexico plans to install **ToITEC** in the coming year, which has filter passbands centered at 150, 220, and 280 GHz, spanning the peak in the kSZ (Bryan et al., 2018)
- **CCAT-prime** will be expected to begin its operations in 2021, and will have a 6-m aperture sub-mm telescope (Stacey et al., 2018); bolometer camera, Prime-Cam covers the range between 190 and 450 GHz, which should have at least an order of magnitude improvements over the Planck data (Erler et al., 2018)

# Future Experiments

- Various instruments on the **ACT** and **SPT** will allow them to detect thousands of SZ selected clusters (Benson et al., 2014; Henderson et al., 2016)
- The Atacama Large Aperture Submm/mm Telescope (**AtLAST**) aims to build a 50 m single dish observatory (Bertoldi, 2018); serve as a complement to the lower-resolution CMB primary anisotropies and SZ survey telescopes
- **Vera C. Rubin Observatory** (formerly LSST) allows for the measurement of highredshift samples, due to a large increase in S/N (Ivezić et al., 2019); measurements of the non-linear regime through weak lensing, as a probe for the uncertainty in processes related to baryons

# Future Experiments

- The Chajnator Sub/millimeter Survey Telescope (**CSST**) plans on building an inexpensive 30 m single dish survey telescope based between 90-420 GHz, based on the design by Padin et al. (2014); provide extremely deep SZ maps for a large sample of clusters
- Space based missions, such as Cosmic Origins Explorer (**CoRE**) (Delabrouille et al., 2018) and Probe of Inflation and Cosmic Origins (**PICO**) (Sutin et al., 2018) could enable an increase in the number of detected SZ clusters

# Conclusion

- The **thermal and kinematic SZ effects**, first theorized in the 70s, have matured in the experimental, observational, and theoretical fronts, including the full spectral measurement of the tSZ and pairwise kSZ signal detections
- The theory, applications, extraction methods, and history of tSZ and kSZ measurements were reviewed
- Current and future experiments will allow us to **probe more clusters** and allow for more kSZ detections in **cross-correlation studies**, allowing us to further place constraints on cosmological models and the finer properties of the ICM
- **Next decade** of SZ effect measurements particularly exciting in several avenues from the cosmological scales to galaxy scales